FINAL REPORT

A Three Dimensional Analysis
of Gas Flow Distribution
in the Drying Zone of a
Pellet Induration Furnace

IRON ORE COOPERATIVE RESEARCH SPONSORS

National Steel Company
Inland Steel Company
Eveleth Taconite Company
M. A. Hanna Company
Pickands Mather & Company
USS, Division of USX Corporation
Cyprus North Shore Mining Company
Minnesota Power

University of Minnesota
Natural Resources Research Institute

Minnesota Department of Natural Resources

A Three Dimensional Analysis of Gas Flow Distribution in the Drying Zone of a Pellet Induration Furnace

by

David J. Englund
Minnesota Department of Natural Resources
Division of Minerals
Hibbing, Minnesota

Prepared for the Iron Ore Cooperative Research Committee
June 23, 1993

TABLE OF CONTENTS

Summary 1
Introduction 2
Why a CFD Study? 2
Eveleth Taconite Furnace 3
Model Assumptions 4
2D Model 4
Comparison of 2D and 3D Solutions 5
Discussion of 3D Simulations 6
Pot-Grate Test Results 8
Preheat Quench Tests 8
Fired Pellet Tests 9
2D Baffle Simulations 10
Model Validation 10
Conclusions 12
References 13

TABLES:
Table 1. Pot-Grate Preheat Quench Test Results 14
Table 2. Pot-Grate Fired Pellet Test Results 14
Table 3. CFD Simulation - Mass Flow Results 15
Table 4. Eveleth Taconite Furnace Temperature Survey 16

FIGURES:
Figure 1. CFD Problem Definition 17
Figure 2a. Grate-Kiln Indurating System 18
Figure 2b. Eveleth Taconite Drying Zone 19
Figure 3. 2D Grid Series 20
Figure 4. Gas Temperature Profile at Pellet Bed Surface . . 21
Figure 5. Vertical Gas Temperature Profile 22
Figure 6. Pressure Drop Across Bed 23
Figure 7. Gas Temperature Profile at Inlet Center Line . . 24
Figure 8. Gas Temperature Profile at Bed Surface 25
Figure 9. Pressure Profile at Bed Surface 26
Figure 10a. Gas Temperature Contours - Windbox 4 27
Figure 10b. Gas Temperature Contours - Windbox 4 28
Figure 11. Furnace Drying Zone - 6 Windboxes 29
Figure 12. Gas Temperature Profile at Bed Surface 30
Figure 13a. Gas Temperature - Bed Surface - Original Machine Design 31
Figure 13b. Gas Temperature - Bed Surface - Current Machine Design 32
Figure 13c. Gas Temperature - Bed Surface - Outlet Relocation Modification 33
Figure 13d. Gas Temperature - Bed Surface - Inlet/Outlet Relocation Modification 34
Figure 14. Predicted Gas Mass Flows - Four Simulation Cases 35
Figure 15. Pot-Grate Test Temperature Profiles 36
Figure 16. Pot-Grate Magnetite Oxidation End of Preheat Zone 37
Figure 17. Pot-Grate Compression Strength End of Preheat Zone 38
Figure 18. Pot-Grate Mini Tumble Strength End of Preheat Zone 39
Figure 19. Pot-Grate Fired Pellet Compression Strength . . . 40
Figure 20a. 2D Model Simulation Without Baffles 41
Figure 20b. 2D Model Simulation With Baffles 42
Figure 21. Furnace Thermocouple Port Locations 43

A THREE DIMENSIONAL ANALYSIS OF GAS FLOW DISTRIBUTION IN THE DRYING ZONE OF A PELLET INDURATION FURNACE

Minnesota Department of Natural Resources
Division of Minerals
Hibbing, Minnesota

SUMMARY:

The reader should note that the model validation section at the end of this report was written following the presentation of results at the Duluth AIME Mining Symposium on January 21, 1993. This report has been revised to accommodate the validation discussion; however, model validation is not yet considered complete and further testing will take place during the fall 1993.

A three dimensional computational fluid dynamics (CFD) model of a drying zone in an iron ore pellet grate-kiln induration system has been developed by the Minnesota Department of Natural Resources, Minerals Division. Simulation runs with the model have shown that minimal mixing of gases occurs in cases where multiple gas streams enter a zone at differing temperatures and that the resulting temperature disparities appear responsible for significant variation in pellet physical strength and magnetite content developed in the preheat zone on the grate.

Pot-grate tests using simulation temperature profiles for which gas temperatures varied by as much as 350 deg C across the grate demonstrated that gas temperatures can significantly impact pellet properties. The results showed a 20% increase in magnetite content and a 50% decrease in compression strength in pellets at the bottom of the bed on the colder side of the grate by end of preheat. The simulation results have also shown this type of modeling to be useful in predicting fan flow rates and in-leakage effects on the grate.

Validation with plant operating conditions was tested on April 14, 1993, by inserting a thermocouple probe into eight sampling ports on the Eveleth furnace. This test confirmed the existence of temperature segregation within the zone, but with smaller gradients than predicted by the model (350 C predicted vs 75-160 C measured). The furnace survey indicated turbulence to be a significant factor and modifications to the model are in progress to account for greater turbulence effects.

INTRODUCTION:

The Minerals Division of the Minnesota Department of Natural Resources has initiated a CFD modeling research project as a member of the Iron Ore Cooperative Research Committee (IOCRC). The IOCRC is a cooperative effort whose goal is to improve the operating efficiency of the Minnesota taconite mining industry. Committee representatives include all seven Minnesota taconite mining operations, the University of Minnesota, the U.S. Bureau of Mines, and three minerals beneficiation laboratories situated on the Mesabi Iron Range in northern Minnesota.

The state and industry are exploring application of CFD modeling to heat transfer and gas flow conditions within the induration furnaces used for production of iron ore pellets. Specifically, interest in CFD modeling was sparked by a desire to re-examine the "perfect mixing assumption" for gas flow, which is so frequently used to simplify energy and gas flow balances in pellet induration systems. The results discussed in this report do not support the perfect mixing assumption and, in fact, show that under certain conditions significant segregation of mass and energy flow can occur.

The State of Minnesota purchased a CFD software package known as Easyflow from Adaptive Research Corporation in Huntsville, Alabama, which interfaces with the PHOENICS CFD source codes. This package was upgraded with a version called CFD2000, which produced the results discussed in this report. CFD2000 has now been replaced with Phoenics 1.6.6 supported by Cham of North America Atlanta, Georgia. The simulation results presented were performed using a PC 486/50 with 32mb of ram.

CFD, computational fluid dynamics, is a family of computer codes which simulate fluid flow, heat transfer, chemical reaction, and related phenomena, from first principles in one, two, or three dimensional systems. These codes use a variety of numerical techniques for solution of linear and non-linear partial differential equations. A number of publications are listed at the end of the paper for further reference.[1,2,3,4,5] Solution format typically follows a path as shown in figure 1.[6]

WHY A CFD STUDY?

Some mining companies in Minnesota have access to the INDSYS pellet induration simulator, developed by Dr. Mark Cross. In order to set up a simulation, the INDSYS program requires the user have extensive knowledge of gas flow, including leakages, throughout the furnace. INDSYS assumes perfect mixing of two or more gas streams entering a zone at different temperatures, when such conditions occur. Dr. Cross has also been active in CFD analysis for pellet induration systems, and is currently working on a separate program to interface with INDSYS for prediction of gas flow based on pressures at specified nodes in the indurator.[7,8,9,10]

The INDSYS user must estimate gas flow in the furnace from experience, from pot-grate data, or from plant air surveys. But how does the user simulate a condition for which no plant data exists, or a condition where two gas streams enter a zone at significantly different temperatures? How much mixing occurs? How do the flows distribute themselves within the zone? It was toward this end that the research program was directed, to see what a three dimensional gas flow analysis of a pellet induration furnace would reveal. The grate machine operated by Eveleth Taconite Mining Company presented a perfect opportunity, where, within the drying zone, 780 deg C recoup gases mix with 350 deg C preheat fan gases.

The goals for this CFD evaluation are two-fold; first to demonstrate how CFD analysis will enhance understanding of gas flow in the machine and, secondly, to demonstrate how the CFD approach allows plant operators to simulate different duct inlet and fan outlet configurations, possibly including use of deflectors or baffles within the furnace. The results of these types of CFD simulations enable the INDSYS user to quantitatively detail gas flow input required by INDSYS for simulation. By running INDSYS, the impacts of the proposed configuration on fuel consumption and production rate can be determined, providing the necessary data for cost/benefit analysis.

EVELETH TACONITE FURNACE:

Eveleth Taconite Company participated by allowing access to plant data and machine specifications. Throughout the report reference will be made to the A side and the B side of the drying zone. The A side is the side in which the 1A preheat fan flow enters the zone in windboxes 1-3 and high temperature recoup gas enters in windboxes 5-6. While on the B side, the 1B preheat fan flow enters in windboxes 3-5. Figure 2a shows a typical grate kiln indurating system, and figure 2b shows the detail of the 3D model grid. Originally, recoup gas also entered through an inlet in windbox 4; this inlet is currently closed.

The recoup inlet in windbox 4 was closed to correct a grate casting wear problem. The Eveleth machine experiences higher casting wear on the B side of the grate. In 1984 Eveleth personnel ran tests by inserting thermocouples in the pellet bed. The thermocouples were placed about 1 meter in from each side of the machine. The temperature profiles generated as the thermocouples travelled with the grate recorded higher gas temperatures on the A side in windboxes 4-6. The windbox 4 inlet was closed off to force recoup air across to the opposite side of the grate from remaining inlets in windboxes 5 & 6. The simulations to be discussed will show that this desired effect is not achieved when the recoup inlet to windbox 4 is closed.

A crude three dimensional CFD model was developed in late 1991. It did reveal temperature segregation within the zone, and the simulation data qualitatively correlated with the 1984 plant data. The results encouraged continuation of the study, and the project moved forward under the sponsorship of the Iron Ore Cooperative Research Committee.

MODEL ASSUMPTIONS:

In these models pressures are fixed at all inlets and outlets. Values are specified based on plant operating data. Gas flow results from pressure differential in the system. The pressure drop across the bed is simulated as a resistance to flow using standard internal PHOENICS variables. Furnace walls are considered adiabatic. Leakages were incorporated above and below the bed on the pellet feed end, above the bed at the drying zone/preheat zone separation, and above and below the bed along both sides of the furnace. The side leakages are based on the geometry of side casting doors, using a 1.2CM slit above and below the bed in each windbox. The end leakages are based on known furnace wall clearances. The models are single phase, that is, only physical and thermodynamic properties of the gas are taken into account. If necessary, two phase flow could be incorporated to detail heat transfer and chemical reactions occurring in the bed.

The bed is simulated by a region functioning as a heat sink with resistance to flow. The magnitude of the heat sink was determined from an INDSYS simulation; this term is normalized as heat loss per unit bed volume. For the simulations presented, enthalpy changes in the off gas due to evaporation of moisture from the pellet bed to the gas stream have not been taken into account. The heat sink term is based solely on net heat transferred to the pellet bed. Flow resistance was empirically determined; future development can and should relate it to bed permeability.

2D MODEL:

Because of the extensive computation time required for three dimensional analysis using a PC 486 (about 20-30 hours per simulation), initial development took place using a 2D model format. This format simulates flow in a cross sectional plane centered in windbox 4 when the recoup inlet is open.

In CFD analysis the number of cells in the solution grid determine accuracy of the solution. The trade off with increasing numbers of cells is computation time. With the 2D model a number of different cell densities within the computation grid were evaluated to determine grid size where the solution became grid independent. That is, where no further change in solution occurred with addition of more cells. Convergence was judged by following recommended software criteria.

For the 2D model, grids ranged from 20x40 to 100x120 (wxh) cells and respective computation times ranged from 8 minutes to 95 minutes. The 3D model uses a 24x54x61 (wxhxl) grid in contrast. From the 2D work, the 80x100 grid provided acceptable grid independence when judging total mass flow in the system. However, even the 20x40 grid provided very good qualitative representation of temperature profiles in the zone. The impact of grid size on mass flow in the system is shown in figure 3.

Figure 4 compares the five grid sizes using temperature profiles at the bed surface, one can see there is little difference between them, the largest differences occur in regions of steep gradient, such as the edges where in-leakages are present and in the temperature transition region between the two gas streams. The effects of leakage penetrate as far as 0.4 meters in from the source for the coarse grid, by adding more cells the effects are discernable up to 0.2 meters in from the source.

Figure 5 shows the variation in temperature profile vertically from top to bottom of furnace; note how the number of cells in the bed region affect gas temperature upon exiting the bed. Comparing the 20x40 to the 100x120 grid, the off gas temperature below the bed drops by as much as 100 degrees C for the same bed conditions. Pressure profiles also differed mainly in magnitude as shown in figure 6.

COMPARISON OF 2D AND 3D SOLUTIONS:

Comparing the 2D model output with the 3D model output under identical boundary conditions shows good correlation between the grid independent 2D model and the coarser, less well defined solutions of the 3D model.

Figure 7 compares gas temperature profiles along an imaginary centerline across the furnace from inlet face to inlet face. While the width of the temperature gradient differs between the models, both show the gradient between the gas streams very distinctly. The temperature profile across the windbox at the bed surface can be seen in figure 8. Here again the 3D model results differ slightly in magnitude and location, but nonetheless predict the gradient. The steep gradients on the edges are the result of simulated leakage entering through side casting doors. Note how the width of the temperature gradient decreased from approximately 1.5 meters to 0.3 meters, with the increased number of cells in the 2D model.

Figure 9 shows a similar comparison for pressure at the top of the bed moving across the machine. Again the curves are similar, differing about 250 pascal in magnitude.

Figures 10a&b show predicted temperature contours for both the 2D and 3D models in cross section. Gas velocity vectors are shown in the 3D model cross section for reference. The vectors for the 2D model run are identical, but were not shown because they obscure the temperature contours.

At this point, convinced that while the 3D model may not be giving precise absolute values, the results were certainly qualitatively acceptable. So three additional runs using the 24x54x61 grid were conducted.

DISCUSSION OF 3D SIMULATIONS:

The software post processor allows viewing of the results in two or three dimensions. Figure 11 provides a three dimensional isometric view showing gas temperatures at the furnace walls. The confinement of high temperature recoup gas is obvious in this view. Based on the 2D model studies and the 3D simulation of the original furnace design, it appears that where inlets oppose each other, resulting flow conditions restrict movement of gas across the grate. Such that in reaching the center of the grate, horizontal movement ceases and flow continues only vertically down through the bed.

The four simulations are described as follow:

> Case 0: The **original machine** design with all windbox inlets open; inlets from preheat fan 1A in windboxes 1A,2A,3A, inlets from high temperature recoup gas coming from the cooler in windboxes 4A,5A,6A, and inlets from preheat fan 1B in windboxes 3B,4B,5B; waste gas fan 2A exhausting windboxes 1A,2A,3A,4A, and waste gas fan 2B exhausting windboxes 1B,2B,3B,4B.

> Case 1: The **current machine** design with windbox 4 inlet from high temperature recoup flow closed (high temp recoup inlets in 5A,6A). All preheat fan and waste gas fan inlets/outlets remain unchanged.

> Case 2: Relocation of waste gas 2B outlets from windboxes 3B,4B to windboxes 5B,6B. Inlets from 1A preheat fan in 1A,2A,3A, inlets from high temp recoup in windboxes 4A,5A,6A, and inlets from 1B preheat fan in windboxes 3B,4B,5B; waste gas fan 2A exhausting from windboxes 1A,2A,3A,4A and waste gas fan 2B exhausting from 1B,2B,5B,6B.

> Case 3: Outlet relocation as in Case 2, additionally the inlet from 1B preheat fan in windbox 5B was moved to windbox 2B. Inlets from 1A preheat fan in windboxes 1A,2A,3A, inlets from high temp recoup in windboxes 4A,5A,6A, and inlets from 1B preheat fan in windboxes 2B,3B,4B.

Predicted temperature profiles at the center of the grate, along the length of the zone, provide a convenient means for comparison of the four runs. The current furnace configuration shows minimal effect of recoup gas at the center of the grate. By opening the recoup inlet in windbox 4A, and by closing the 1B preheat inlet to windbox 5B, a substantial increase in temperature is achieved as recoup flow penetrates further into the machine. These effects are illustrated in figure 12.

Figures 13a-d provide a comparison of the four runs, showing gas temperature contours at the bed surface. Note the differences in temperature contours in windboxes 4-6 for the various cases. Note how the high temperature region at the pellet bed surface is reduced when the recoup inlet to windbox 4 is closed (Case 0 vs Case 1) and also note that while relocation of outlets opposite the recoup inlets in windboxes 5 & 6 help marginally (Case 0 vs Case 2), it is not until the opposing flow from preheat fan 1B in windbox 5 is eliminated, that the B-side is significantly heated up (Case 3).

Figure 14 and table 3 show relative gas mass flow splits between preheat fans 1A and 1B, and recoup for the four simulations. From this study, Case 3 provides the best balance between the preheat fans and maximizes the recoup flow. Note how total flow to the zone remains relatively constant, while the component flows change relative to each other. For the original design (Case 0), the current design (Case 1), and the outlet modification design (Case 2), the 1A preheat fan flow is 15-20% greater than the 1B preheat fan flow; only for the fully modified case (Case 3) are the 1A and 1B fan flows balanced. The results also show that recoup flow was minimized by closing windbox 4 inlet. Recoup flow was maximized by opening the windbox 4 inlet and eliminating the opposing flow from the 1B preheat fan in windbox 5.

Assuming simulation results were correct, two questions were asked:

> First, what impact on pellet quality and production rate does this temperature disparity have?
>
> Second, if the affects on pellet quality are discernable from one side to the other, how could the machine be modified to yield a more uniform gas and temperature distribution across the machine?

To address the first question, three series of pot-grate tests were performed at the Midland Research Center located in Nashwauk, Minnesota. The objective was to quantify affect of drying zone temperature profile on greenball moisture evaporation, magnetite oxidation, and on fired pellet quality. Pot-grate tests provide a laboratory scale means for simulating induration furnace temperature profiles and gas flows on plant produced greenballs.

Addressing question two, simulation cases 2 & 3 were performed to test potential modifications and their impact and to evaluate the sensitivity of the software to predict changes in flow based on these modifications.

POT-GRATE TEST RESULTS:

National Steel Pellet Company located in Keewatin, Minnesota, provided the greenballs for the pot grate tests. Eveleth Taconite greenballs would have been used had the plant been operating at the time of the pot-grate testing. Tables 1 and 2 summarize the results of the test program.

The variable in the pot tests was temperature; all zone times and pressures were kept constant. The drying zone was broken into six sub-zones, for which temperatures were varied according to predicted profiles (see figure 15). All temperature profiles for preheat and firing zones were held constant, the only variation among the three series was the drying zone temperature profile. Drying and preheat quench tests were carried out in duplicate and the results averaged; nitrogen gas was used to quench the oxidation tests. As it turned out, drying was complete by the end of the zone for all three cycles tested and is not discussed further.

Two of the drying zone temperature profiles were taken from the A-side of the zone, one from the original design simulation (Case 0) with windbox 4 open (cycle C), and one from the current machine design simulation (Case 1) with windbox 4 closed (cycle A). The third series drying zone temperature profile came from the B-side, and represents both original and current design simulations as they yielded nearly identical profiles on this side (cycle B). The profiles exist at one meter in from each side of the furnace in the CFD simulations.

PREHEAT QUENCH TESTS:

Magnetite oxidation shown as percent of total greenball ferrous iron remaining at the end of the preheat cycle was clearly affected by the differences in the drying temperature profiles. These results are shown in figure 16. The pellet ferrous iron content increased as the temperature profiles decreased in intensity. The original A-side profile (cycle C), had the least ferrous iron remaining ranging from 29% near the top of the bed to 35% near the bottom of the bed, followed by the current A-side profile (cycle A), in which ferrous iron ranged from 32% to 49%, while the current B-side profile (cycle B) had the most ferrous iron remaining ranging from 36% to 54%. The most significant changes in ferrous iron content were found in the pellets at the bottom of the bed.

Magnetite oxidation is the subject of another Iron Ore Cooperative Research Study which has shown that pellet physical strengths are greatly affected by both the rate of oxidation and the time/temperature profiles at which the oxidation occurs. Our study did not attempt to optimize the oxidation pellet strength relationship, but only demonstrate that magnetite oxidation in the preheat zone is, in part, dependent on the gas temperature profile experienced by pellets in the drying zone.

Compression strength at the end of preheat was greatest for cycle C, ranging from 46 kgs at the bottom of the bed to 52 kgs at the top of the bed, decreasing as temperature intensity decreased, for cycle A, from 29 kgs to 48 kgs respectively, and for cycle B, from 26 kgs to 46 kgs. There was little variation in strengths at the top of the bed, but considerable variation among pellets in the lower half (center/bottom) of the bed as seen in figure 17.

The mini-tumble test is another measure of pellet strength and was performed on bed composites from the preheat quench tests. This test tumbles a pellet charge in a partitioned ASTM tumble drum and measures breakage after 200 revolutions. Figure 18 shows that abrasion strength has same relation to drying temperature profile as compression strength, that is, as the profiles became progressively colder, pellet resistance to breakage and abrasion decreased as measured by percent weight plus 6.3mm, %wt-6.3mm+28m and %wt-28 mesh. It is desirable to maximize the material retained on the 6.3mm size after tumbling. From table 1 the range was 64%wt +6.3mm to 48%wt to 41%wt for cycle C, cycle A, and cycle B, respectively.

FIRED PELLET TESTS:

Looking at fired pellet quality, the picture becomes a bit more complicated. The cycle B profile yielded the highest compression strengths for fired pellets, while cycle C yielded the lowest compression strengths. Observations of pellet bed thermocouples showed the highest peak temperatures in the bed occurring with the coolest drying zone temperature profile, and the lowest peak temperatures in the bed occurring for the hottest drying zone profile. Peak temperatures are no doubt related to magnetite content remaining at the end of preheat. The remaining magnetite which oxidizes during firing, raises peak firing temperatures in the bed, temperature increasing with the quantity of magnetite being oxidized. The greatest variation of compression strengths occurred for cycle B. The percentage of pellets breaking under 136 kgs (300 lbs) also exhibited some variation with firing cycle, indicating that magnetite oxidation has a pronounced effect on this parameter as well. We saw larger fractions of pellets breaking under 136 kgs in cycles C and B than with cycle A which had the lowest percentage. In cycles C and B oxidation rates were faster and slower, respectively, relative to cycle A. Fired pellet compression strengths are shown in figure 19.

Extrapolation of pot grate results to kiln fired plants is tricky at best, because the pot-grate apparatus cannot simulate the segregation of gas and solids and the tumbling/mixing action that occurs in the kiln. But the results demonstrate that drying zone temperature conditions seem to impact on pellet physical quality throughout the process. Tumble strength and reducibility properties were not affected by the drying temperature profiles in these tests.

2D BAFFLE SIMULATIONS:

The 2D model was also used to look at some internal baffle arrangements. We hoped that placement of baffles would improve gas mixing above the pellet bed. We were unable to identify any passive baffle arrangement capable of completely mixing the gases. One arrangement achieved partial success by deflecting 1B preheat gases downward as they enter on the B-side. This solution does not eliminate the temperature disparity, but merely confines it closer to the furnace wall. Figures 20a&b compare 2D simulations for similar conditions with and without baffles present.

Hanging plates were simulated near the inlet face to stop the horizontal gas momentum. The first and top most plate is located 0.5 meters in from the inlet face and extends 0.66 meters down from the furnace ceiling. The next plate is 1.0 meter in from the inlet face and extends 0.66 meters down from the first plate. The third and lowermost plate is 1.83 meters in from the inlet face and extends down yet another 0.66 meters. This baffle arrangement reduced the preheat inlet flow by 35%, and increased recoup flow by 30% relative to the same boundary conditions without baffles.

MODEL VALIDATION:

The results discussed thus far were based on model simulations generated between November 92 and February 93. On April 14, 1993, a temperature survey was made of the Eveleth furnace drying zone. Temperatures within the drying zone were manually recorded at eight sample points in the zone. Sampling ports were installed prior to the April start-up and can now be used at any time. A schematic showing location of the points is shown in Figure 21. The ports are located on the roof of the furnace.

A thermocouple probe was inserted through the port and lowered to a specific depth in the furnace. The probe consisted of a type K thermocouple with an unshielded junction. It is approximately 12 feet long. The probe was marked in one foot intervals and temperatures were recorded at those intervals, measured from the internal face of the furnace ceiling.

The level of turbulence in the furnace was quickly found to be considerably more significant than had been represented in the model. The reference to turbulence in the furnace at this time is somewhat subjective, being based on the force of pulses felt on the probe, and noted as large, rapid fluctuations in gas temperatures at the sampling point. For this survey approximate minimum and maximum temperatures were manually recorded at each sampling point and thermocouple location. Only at thermocouple location A (TC-A), did the temperature stabilize to a constant value; at the remaining locations the temperature could change as much as 200 F within 5-10 seconds. The probe was held at each sampling point for approximately 90 seconds.

The recorded temperatures are listed in Table 4 (top half), showing that temperature gradients exist within the furnace, but that turbulence dampens the gradients when compared to the model predictions (Table 4 bottom half). Looking at the average of the minimum and maximum values given in Table 4, the following results confirm the existence of a gradient and indicate that further refinement is necessary in the turbulence parameters used in the model.

RANGE OF TEMP GRADIENTS FROM SIDE TO SIDE OF FURNACE

Windbox	Approx. Meas. Gradient	Predicted Gradient
4 TC C/D	40-135 Deg C	20-50 Deg C
5 TC E/H	75-160 Deg C	360-370 Deg C

(ports located about 1 meter in from side walls see fig. 21)

The range of gradient values were found by comparing points at equal distance from the ceiling for thermocouple locations on opposite sides of the windbox. The predicted gradient values came from grid cells located as close to the actual sampling point as the model grid would allow. The CFD grid locations at centers of cells might vary from the actual sample points by up to 0.5 feet.

Comparing results along the length of the grate, significant temperature gradients occur over the distance of one windbox (3 meters) and the larger gradients are found on the B-side which appears to receive the least impact from recoup gases entering on the A-side in windboxes 5 and 6.

RANGE OF TEMP GRADIENTS FROM CENTER WB-4 TO CENTER WB-5

Grate Side	Approx. Meas. Gradient	Predicted Gradient
A-Side TC D/H	71-150 Deg C	310-350 Deg C
B-Side TC C/E	130-250 Deg C	360-370 Deg C

Preliminary runs with the 2-D model have shown that increasing turbulence in the simulations tends to reduce the temperature gradient across the machine, moving the predicted results closer to the measured results. However, attempts to incorporate more turbulence in the 3-D models has led to unstable runs. Presently, attempts are being made to overcome the divergence, but progress has been slow.

Because of the wide and rapid temperature variations, at least one more survey should be conducted in the coming fiscal year (FY94). For this survey, temperature logging and recording will be carried out automatically so that mean temperatures and temperature distributions about the mean can be analyzed. However, before making this survey the turbulence parameters in the 3-D model will be revised and stable runs obtained with which to compare plant data.

CONCLUSIONS:

Upon performing the temperature survey on the Eveleth furnace, the existence of temperature/gas segregation has been shown to exist, but to a lesser extent than originally predicted. It is presumed that the differences are attributable to the role of turbulence in the furnace. Indicating the need for refinement of turbulence parameters in the model. Work is presently underway to incorporate these effects into the model, this work will be continued in FY94. Additional temperature surveys are planned when model revision is complete.

Three dimensional analysis of pellet induration systems using CFD software is feasible and of value as a research tool for re-evaluating gas flow mixing in the furnace. The mass flow data generated from the CFD runs, can provide additional insight in setting up data files for INDSYS runs, particularly when evaluating conditions where no plant data is available.

The pot-grate series performed demonstrate that impact on pellet quality can be quantified for CFD simulation conditions, and effects on energy consumption and production rate can be found by making INDSYS runs. The predictive capabilities for modeling pellet induration systems are then greatly enhanced if one uses a combination of these three simulation tools.

It is also possible to define variables that measure mass and energy flux moving through the bed. Generating surface contours with these variables would allow the user to easily identify regions of low mass flow or low energy flow, resulting from the modifications tested.

There are a number of other problems in the indurating system that could also be modeled:

> Optimizing burner placement in preheat zones for fluxed pellet production, to evenly distribute heat to the pellet bed.
>
> Generating a detailed moisture migration contour for the pellet beds in straight grate systems where recondensation can be a serious problem, to evaluate drying cycle efficiencies.
>
> Creating an oxygen concentration map for air injection into kilns, or preheat zones, to predict magnetite oxidation levels.

The solutions to these examples are not necessarily straightforward, but should be possible through user written subroutines added to the source code. Some of the examples may require incorporation of two phase models which also increases the level of complexity. Finally, parametric studies can be carried out to investigate a number of variables on mass flow. For example, how flow and heat are distributed as a function of fan pressure or damper position.

The down side of three dimensional CFD modeling is computing time. In order to achieve any practicality in 3D solution, computation must be moved from the PC environment to a work station environment to reduce solution time.

REFERENCES:

1. Phoenics, Cham Ltd. Uk, Cham North America, - Instruction Manual TR100.

2. S.V. Patankar, Numerical Heat Transfer and Fluid Flow, Hemisphere Publishing Corp., 1980.

3. S.V. Patankar, Computation of Conduction and Duct Flow Heat Transfer, published by Innovative Research Inc., St. Paul, 1991.

4. O.J. Illegbusi, J. Szekely, Computational Fluid Mechanics in Metals Processing, Iron & Steelmaker, Dec. 1991, V.18, No. 12, pp. 23-30.

5. R.T.Bui, Building Useful and User-Friendly Computer Models of Metallurgical Processes, Journal of Metals, Feb. 1992, V.44, No. 2, pp. 16-22.

6. CFD2000 Version 1.01 User Manual.

7. M. Cross, K. C. Wade, Computer Simulation of Iron Ore Pellet Induration with Additives, 5th International Symposium on Agglomeration, United Kingdom, Sept. 1989.

8. M. Cross, M.K. Patel, K.C. Wade, Analysis of the Gas Flow and Heat Distribution in Iron Ore Pellet Induration Systems, Control 90 Mineral and Metallurgical Processing, Salt Lake City, Utah, AIME/SME 1990, pp. 99-106.

9. M. Cross, M.K. Patel, and M. Afzal, Computer Simulation of Pellet Induration for Process Optimization and Control, 64th Annual Meeting, Minnesota Section AIME, Duluth, Minnesota, Jan. 1991, pp. 353-365.

10. M. Afzal and M. Cross, Mathematical Modeling of the Gas Flow Distribution in Iron Ore Pellet Induration Systems, 2nd International Symposium on Modeling in Iron and Steel Industry, Toronto, Canada, April 1992, pp. 367-374.

TABLE 1. POT-GRATE PREHEAT QUENCH TEST RESULTS

	Compression Str. Kgs:				Mini-Tumble % Wt. on:				Oxidation % of Total Fe Remaining:		
	Cycle C	Cycle A	Cycle B		Cycle C	Cycle A	Cycle B		Cycle C	Cycle A	Cycle B
Top-Bed Compression Kgs	53.9	49.4	48.9	% Wt. +6.3mm	64.6	49.4	50.2	Top-Bed Oxidation	29.72	35.16	34.05
	51.7	48.1	44.9		64.0	48.0	32.4		28.27	30.06	39.15
Average	52.8	48.8	46.9	Average	64.3	48.7	41.3	Average	28.99	32.61	36.59
Center Compression Kgs	51.7	47.6	42.2	% Wt. 6.3mm + 28M	11.6	17.6	18.0	Center-Bed Oxidation	34.05	43.47	43.47
	50.8	48.5	39.0		13.4	19.4	29.8		32.98	39.15	43.13
Average	51.2	48.1	40.6	Average	12.5	18.5	23.9	Average	33.51	41.30	43.29
Bottom Compression Kgs	44.0	32.7	29.0	% Wt. -28M	23.8	33.0	31.8	Bottom-Bed Oxidation	34.77	49.30	50.36
	48.5	26.3	24.0		22.6	32.6	37.8		34.77	49.98	57.99
Average	46.3	29.5	26.5	Average	23.2	32.8	34.8	Average	34.77	49.63	54.17

Green Ball Moisture % Wt. - 9.1

Cycle A = Current machine drying zone temp profile - 1 meter from A-side

Cycle B = Current machine drying zone temp profile - 1 meter from B-side

Cycle C = Original machine drying zone temp profile - 1 meter from A-side

TABLE 2. POT GRATE FIRED PELLET TEST RESULTS

	Original A-Side Cycle C	Current A-Side Cycle A	Current B-Side Cycle B
Avg. Compression Str. Kgs	183.2	215.9	209.5
Compression % <136 Kgs	15	8.3	13.3
Std. Dev.	48.0	59.9	63.0
Tumble %Wt +6.3mm	96.6	96.3	96.4
Reducibility R40	0.91	0.88	0.9

TABLE 3. CFD SIMULATION - MASS FLOW RESULTS

	Case 0	Case 1	Case 2	Case 3
PREHEAT 1A FAN FLOW KG/SEC				
Inlet 1A	36.77	38.45	37.09	**31.36**
2A	34.60	37.04	34.59	**29.63**
3A	30.39	35.10	29.91	**28.03**
TOTAL	101.76	110.59	101.59	**89.02**
Gas/Solids*	0.7269	0.7899	0.7256	**0.6359**
% Change**	0	8.68	-0.17	**-12.52**
PREHEAT 1B FAN FLOW KG/SEC				
Inlet 2B	-	-	-	**29.88**
3B	31.13	34.57	31.57	**28.03**
4B	27.33	31.87	26.77	**28.81**
5B	26.82	30.61	26.46	**-**
TOTAL	85.28	97.05	84.80	**86.72**
Gas/Solids*	0.6091	0.6932	0.6057	**0.6194**
% Change**	0	13.80	-0.56	1.69
HIGH TEMP RECOUP FLOW KG/SEC				
Inlet 4A	24.97	-	24.74	26.26
5A	23.58	28.51	23.32	27.21
6A	19.58	21.99	19.2	23.25
TOTAL	68.13	50.50	67.26	76.72
Gas/Solids*	0.4866	0.3607	0.4804	0.5480
% Change**	0	-25.88	-1.28	12.61
WASTE GAS OUTLET KG/SEC (includes leakage)	255.17	258.14	253.65	252.46
1A/1B FLOW RATIO	1.19	1.14	1.20	1.03

* Mass Flow Ratio - simulated solids flow was 504 $\frac{MT}{Hr}$ or 140 Kg/sec

** % change is change relative to Case 0

TABLE 4. EVELETH TACONITE FURNACE TEMPERATURE SURVEY

	Thermocouple Location/Designation																	
	Dist. from Roof (ft.)	WB 1 TC A	WB 4 TC B		WB 4 TC C		WB4 TC D		WB 5 TC E		WB 5 TC F		WB 5 TC G	WB 5 TC H		WB 6 TC 1	
			Min	Max	Min	Max	Min	Max	Min	Max	Min	Max		Min	Max	Min	Max
Meas. Temp Deg F	1	560	950	1050	880	950	950	1020	890	1000	900	970	NA	1130	1200	1370	1400
	2	600	990	1080	850	950	1000	1050	850	900	900	1000		1150	1180	1400	1430
	3	620	900	1000	700	800	900	980	780	950	950	1050		1110	1120	1380	1420
	4	600	790	850	650	800	900	970	800	890	960	1050		1090	1100	1380	1430
	5	570	700	840	600	750	900	950	840	920	980	1040		1060	1070	1380	1420
	6	580	650	790	550	700	830	900	850	950	980	1040		1030	1040	1390	1400
	7	560	650	830	580	650	830	890	890	980	970	1030		1100	1160	1350	1370
	8	550	700	850	600	700	840	920	850	950	930	990		1040	1100	1330	1360
	9	540	790	850	600	700	840	900	880	960	920	950		1050	1150	1320	1340
Temp Deg C	1	293	510	566	471	510	510	549	477	538	482	521		610	649	743	760
	2	316	532	582	454	510	538	566	454	482	482	538		621	638	760	777
	3	327	482	538	371	427	482	527	416	510	510	566		599	604	749	771
	4	316	421	454	343	427	482	521	427	477	516	566		588	593	749	777
	5	299	371	449	316	399	482	510	449	493	527	560		571	577	749	771
	6	304	343	421	288	371	443	482	454	510	527	560		554	560	754	760
	7	293	343	443	304	343	443	477	477	527	521	554		593	627	732	743
	8	288	371	454	316	371	449	493	454	510	499	532		560	593	721	738
	9	282	421	454	316	371	449	482	471	516	493	510		566	621	716	727
Avg Temp Deg C	1	293	538		491		529		507		502			629		752	
	2	316	557		482		552		468		510			629		768	
	3	327	510		399		504		463		538			602		760	
	4	316	438		385		502		452		541			591		763	
	5	299	410		357		496		471		543			574		760	
	6	304	382		329		463		482		543			557		757	
	7	293	393		324		460		502		538			610		738	
	8	288	413		343		471		482		516			577		729	
	9	282	438		343		466		493		502			593		721	
* CFD Model Temp Deg C	1	650	680		680		700		680		681			1050		840	
	2	650	680		680		710		680		683			1050		851	
	3	650	680		680		715		680		685			1050		870	
	4	650	680		680		718		680		687			1050		888	
	5	650	680		680		722		680		689			1050		910	
	6	650	680		680		724		680		691			1050		930	
	7	650	680		680		728		680		693			1049		955	
	8	650	680		680		730		680		693			1048		960	
	9	650	680		680		732		680		693			1043		955	

* CFD temps taken from file FULLDRY2.R10 which simulates machine as of Feb 93 including the steel duct insert in windbox 6.

FIGURE 1

CFD PROBLEM DEFINITION

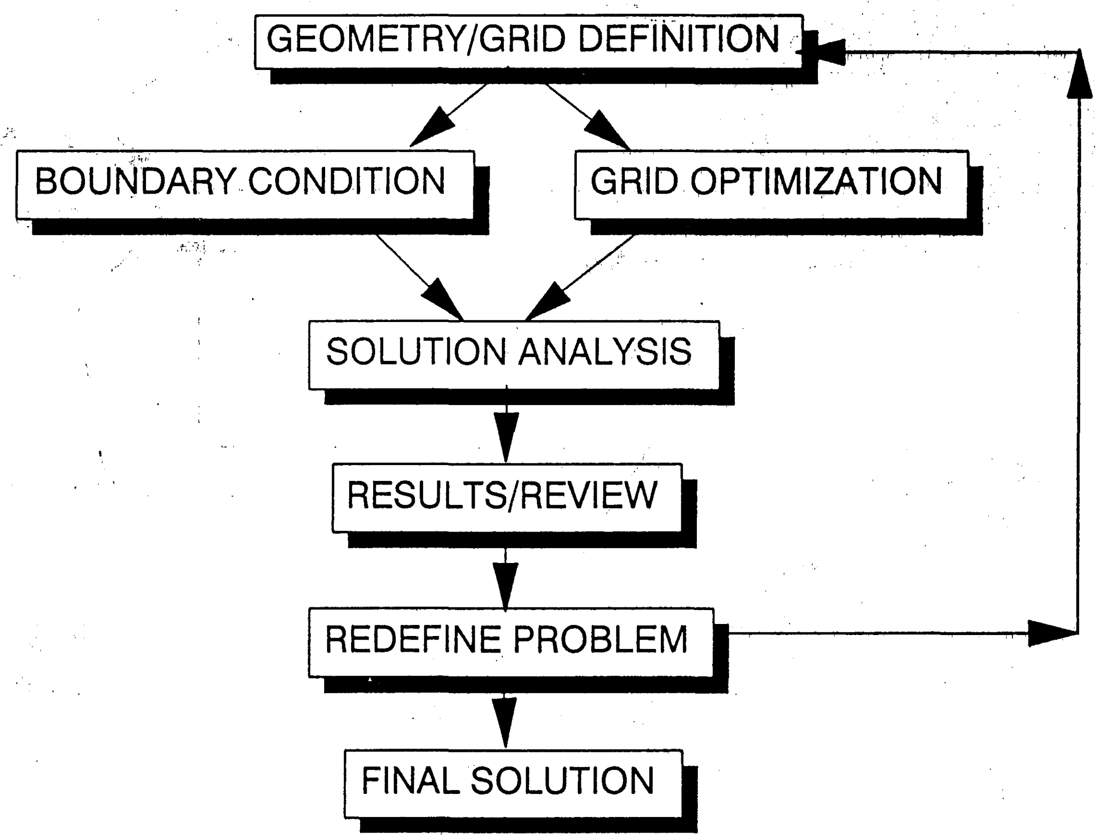

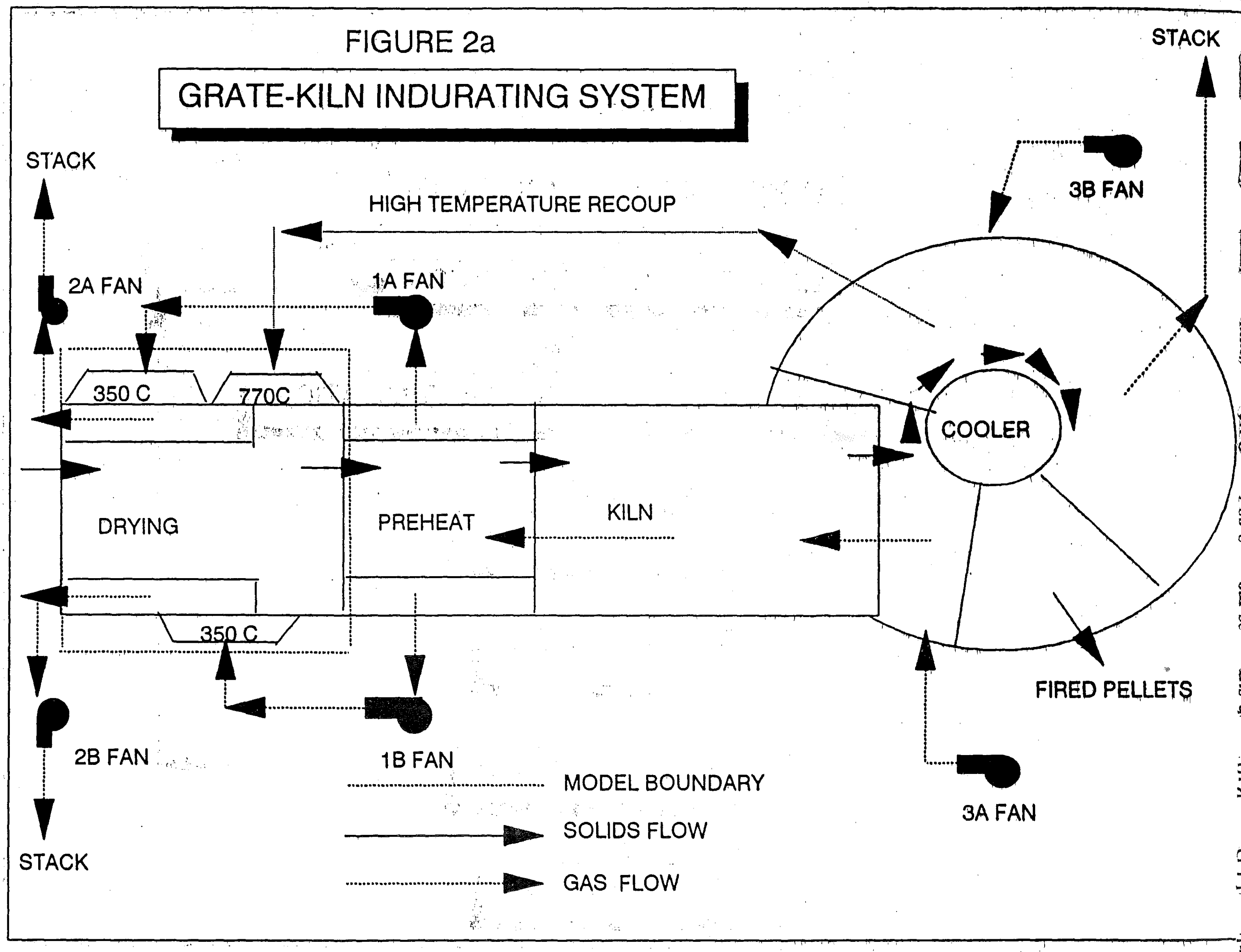

FIGURE 2a

GRATE-KILN INDURATING SYSTEM

FIGURE 2b

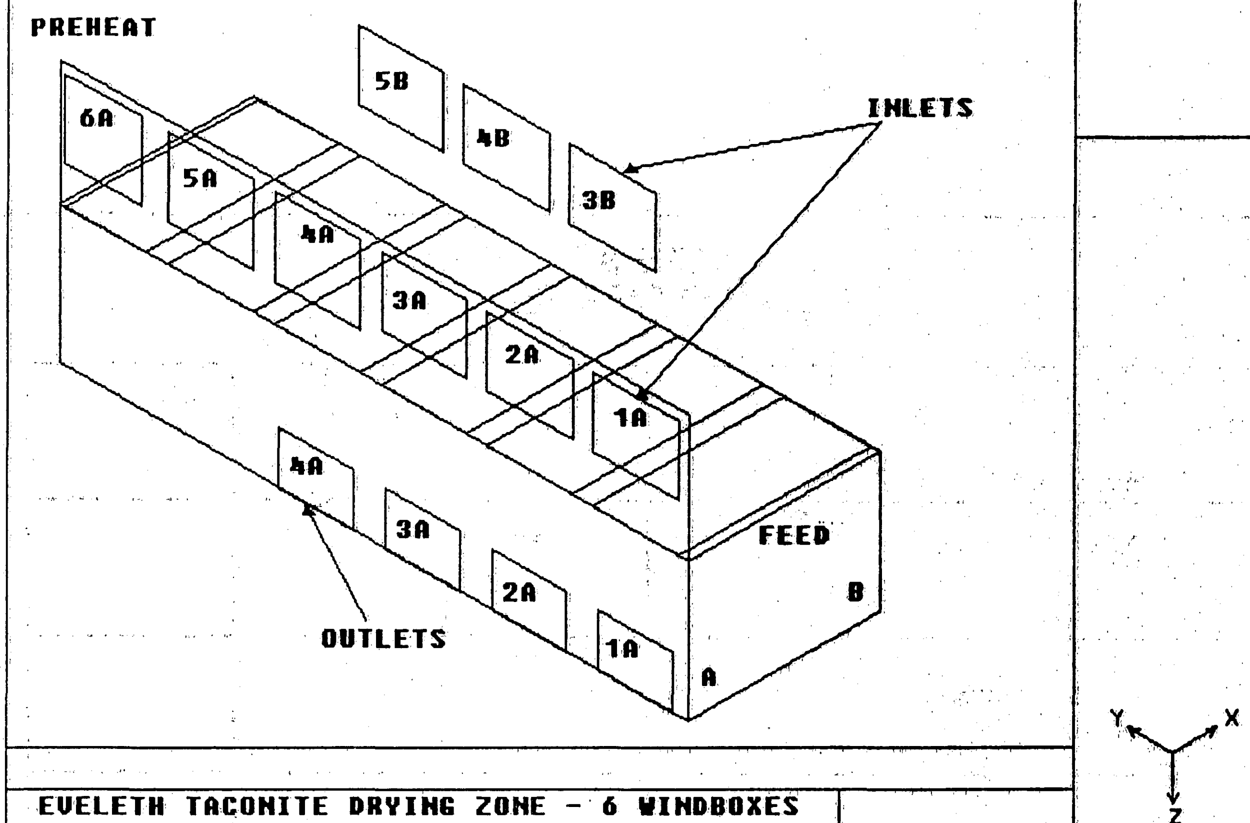

EVELETH TACONITE DRYING ZONE - 6 WINDBOXES

FIGURE 3
2D GRID SERIES

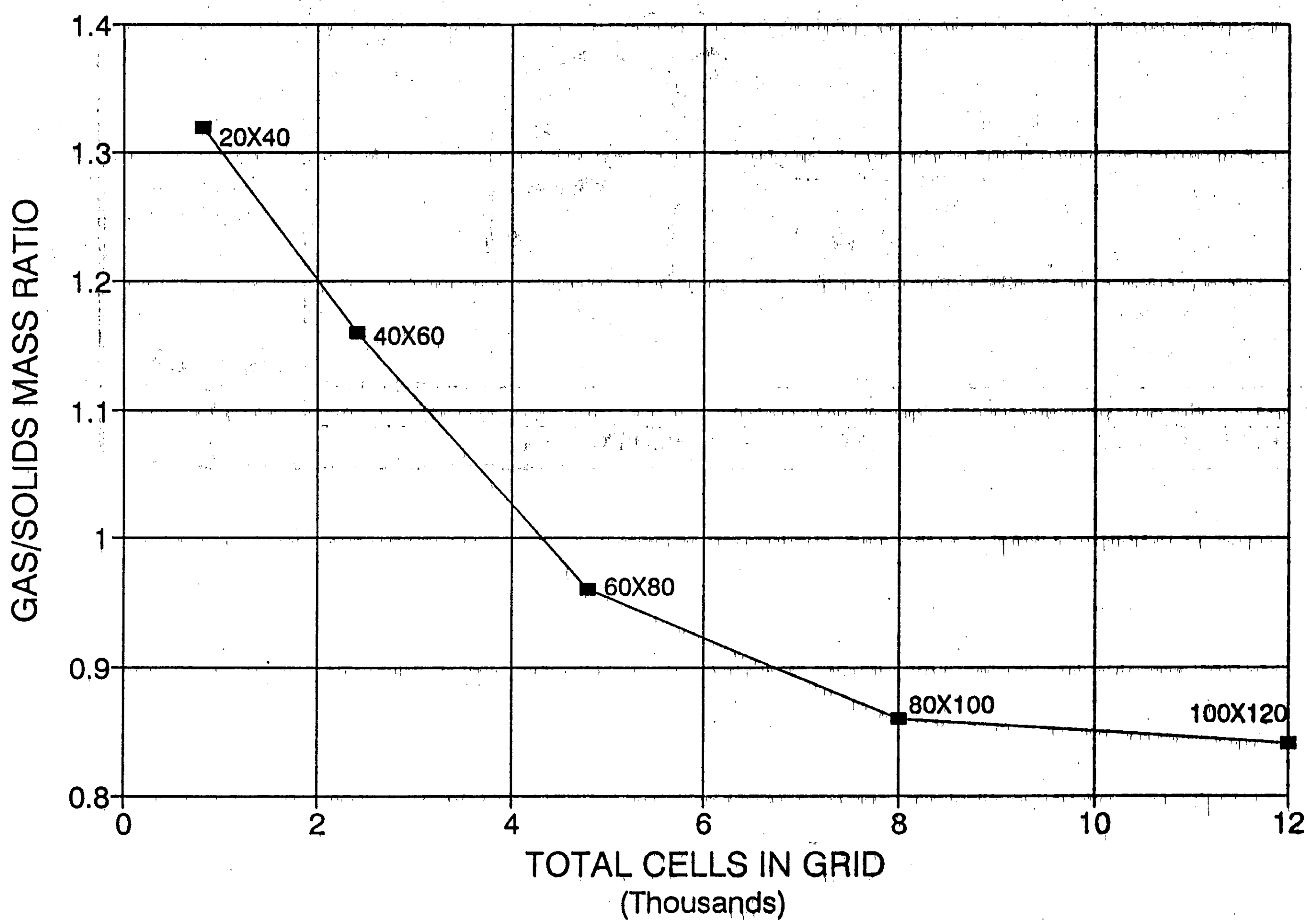

FIGURE 4

GAS TEMPERATURE PROFILE AT PELLET BED SURFACE

(2D GRID SERIES)

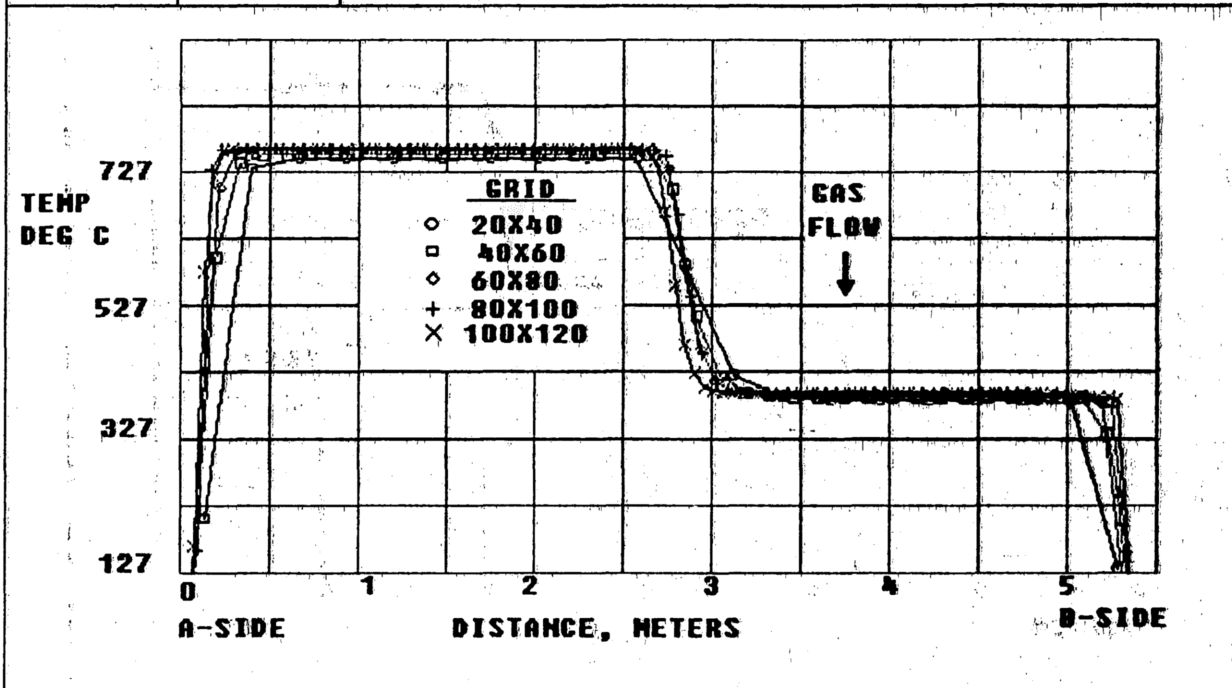

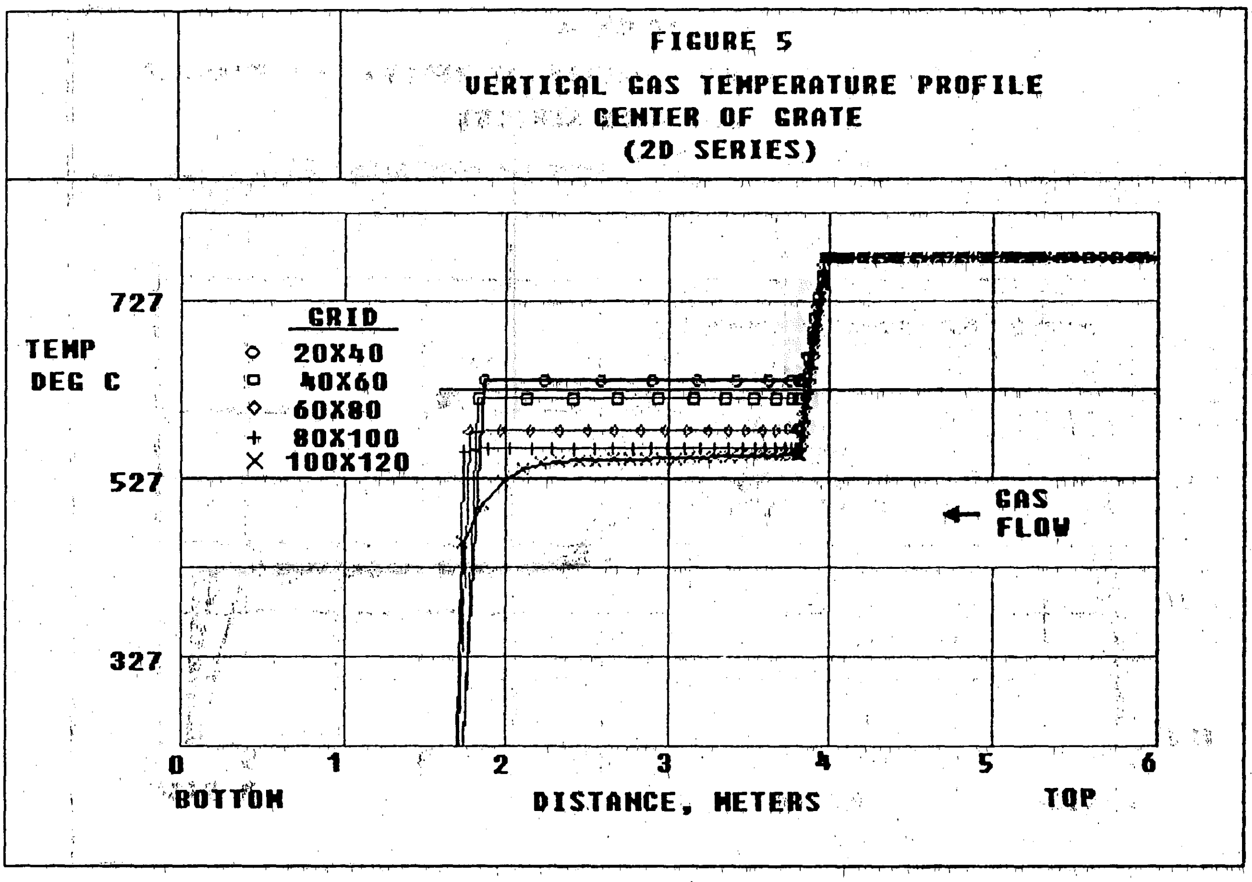
FIGURE 5
VERTICAL GAS TEMPERATURE PROFILE
CENTER OF GRATE
(2D SERIES)
TEMP
DEG C
727
527
327
GRID
20X40
40X60
60X80
80X100
100X120
GAS
FLOW
0
1
2
3
4
5
6
BOTTOM
DISTANCE, METERS
TOP

FIGURE 6
PRESSURE DROP ACROSS BED
(2D GRID SERIES)

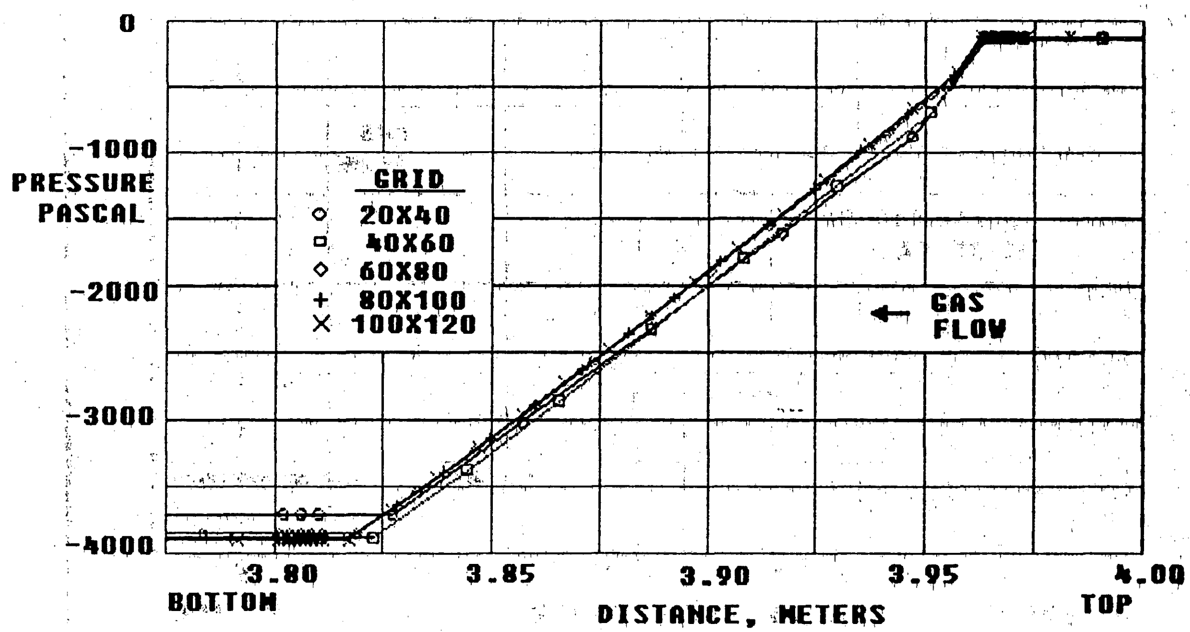

FIGURE 7

GAS TEMPERATURE PROFILE AT INLET CENTER LINE

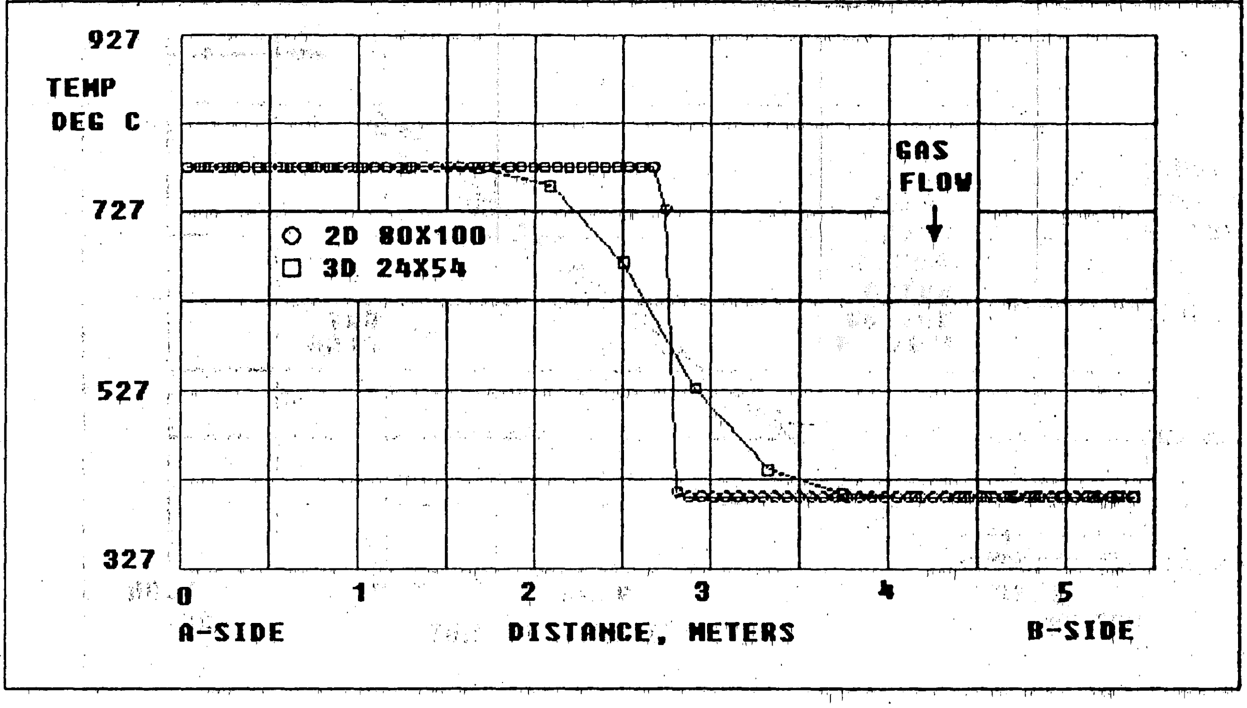

FIGURE 8

GAS TEMPERATURE PROFILE AT BED SURFACE

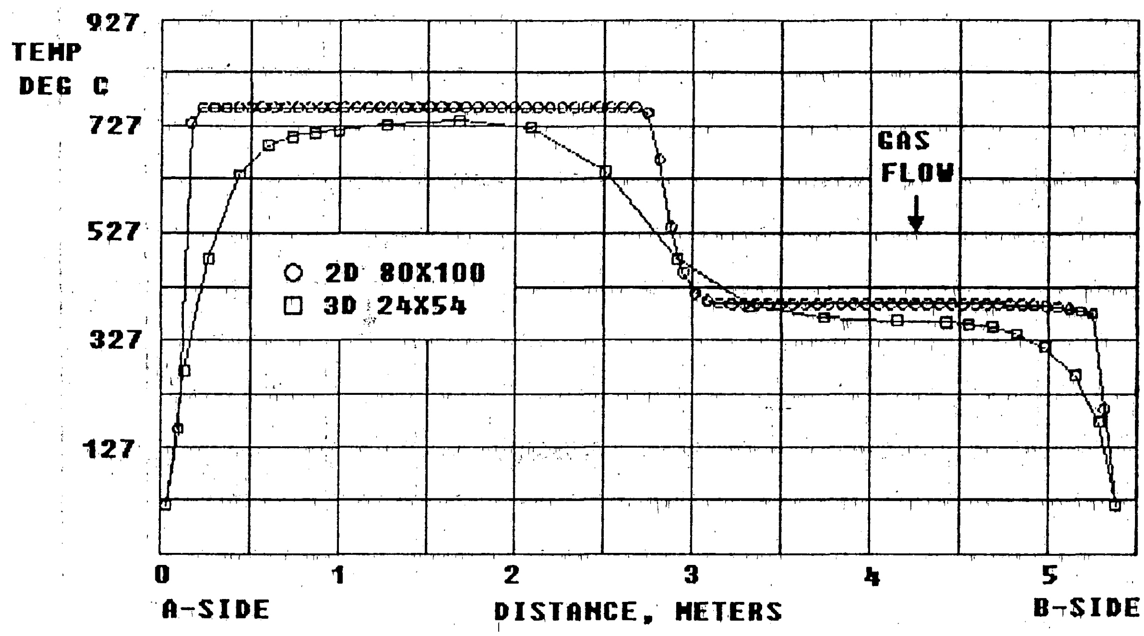

FIGURE 9

PRESSURE PROFILE AT BED SURFACE

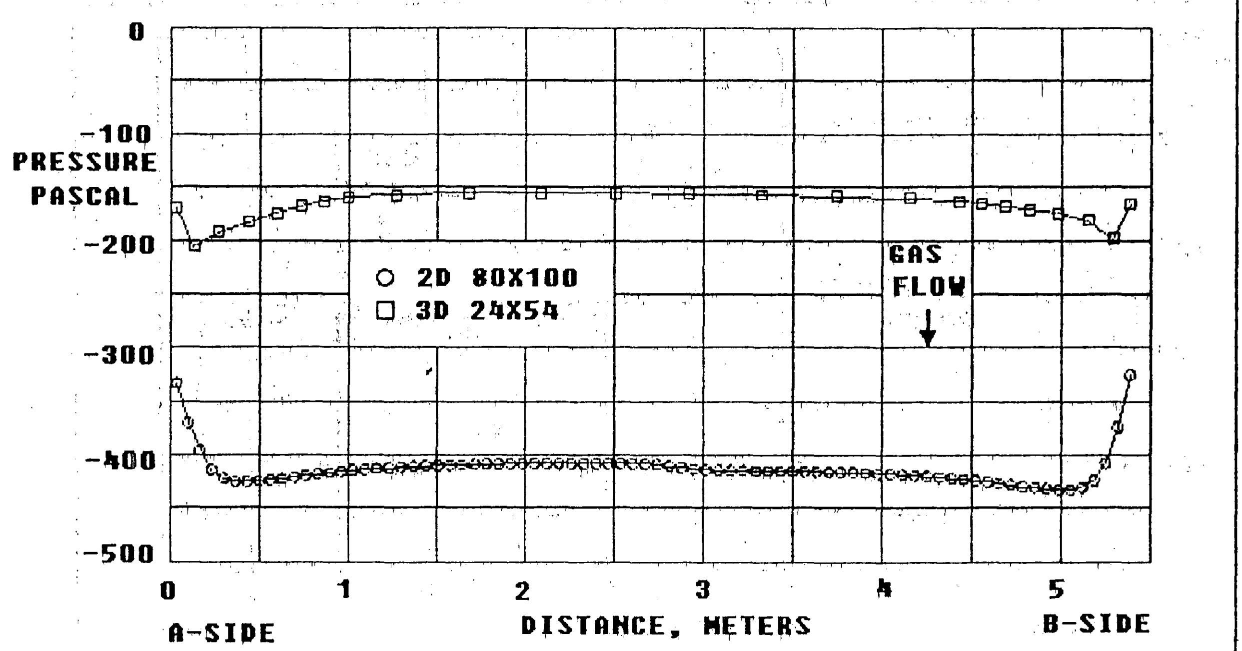

FIGURE 10a

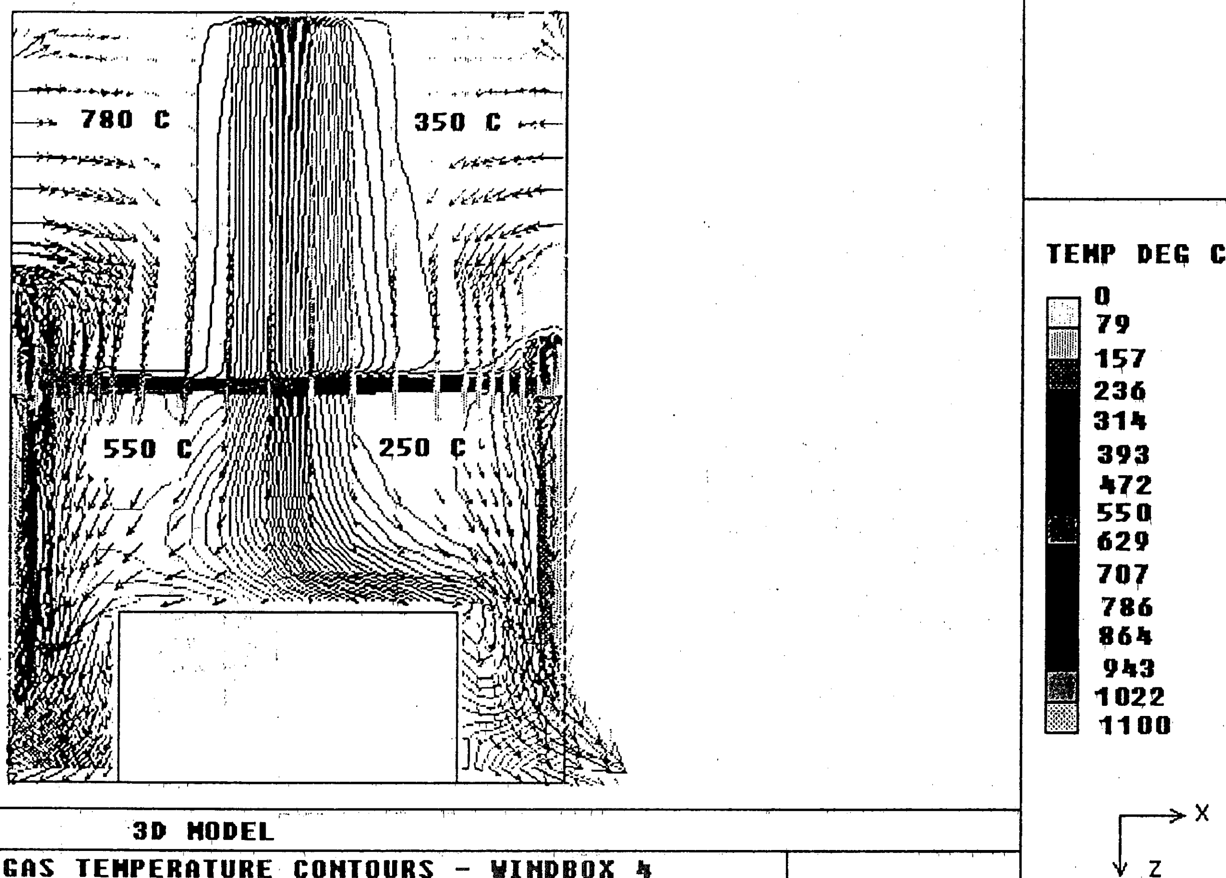

3D MODEL

GAS TEMPERATURE CONTOURS - WINDBOX 4

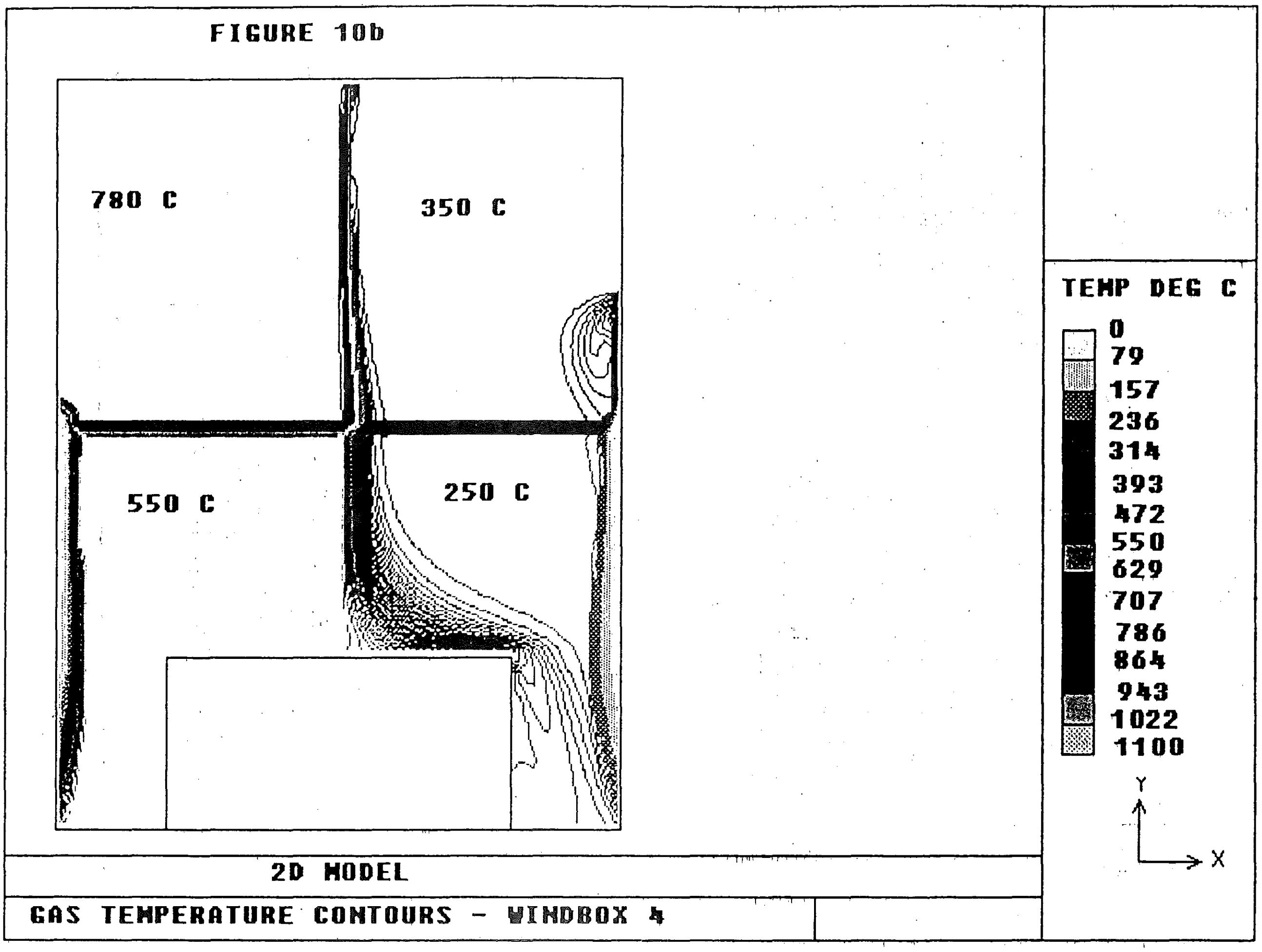
FIGURE 10b
780 C
350 C
550 C
250 C
TEMP DEG C
0
79
157
236
314
393
472
550
629
707
786
864
943
1022
1100
Y
X
2D MODEL
GAS TEMPERATURE CONTOURS - WINDBOX 4

FIGURE 11

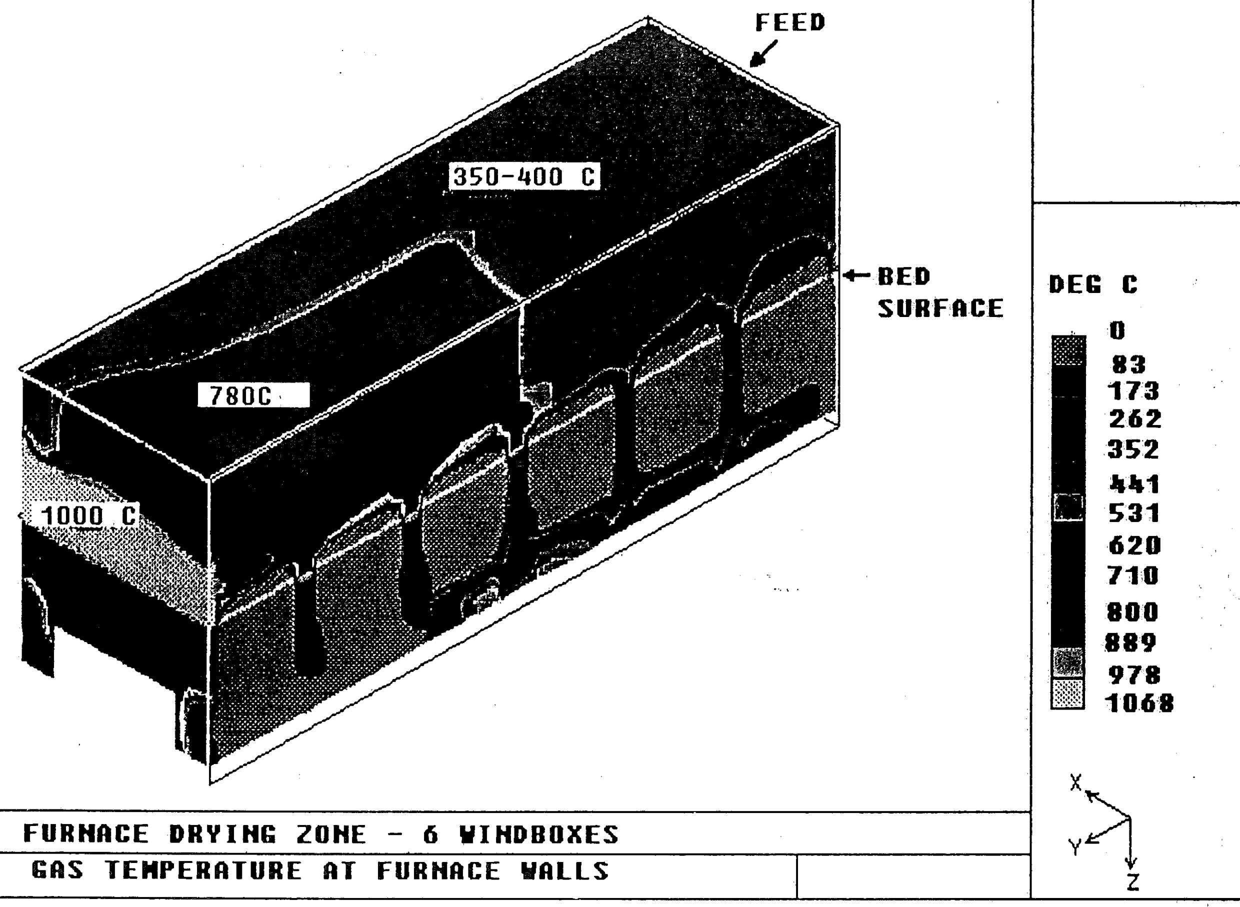

FURNACE DRYING ZONE - 6 WINDBOXES

GAS TEMPERATURE AT FURNACE WALLS

FIGURE 12

GAS TEMPERATURE PROFILE AT BED SURFACE
ALONG CENTER OF GRATE

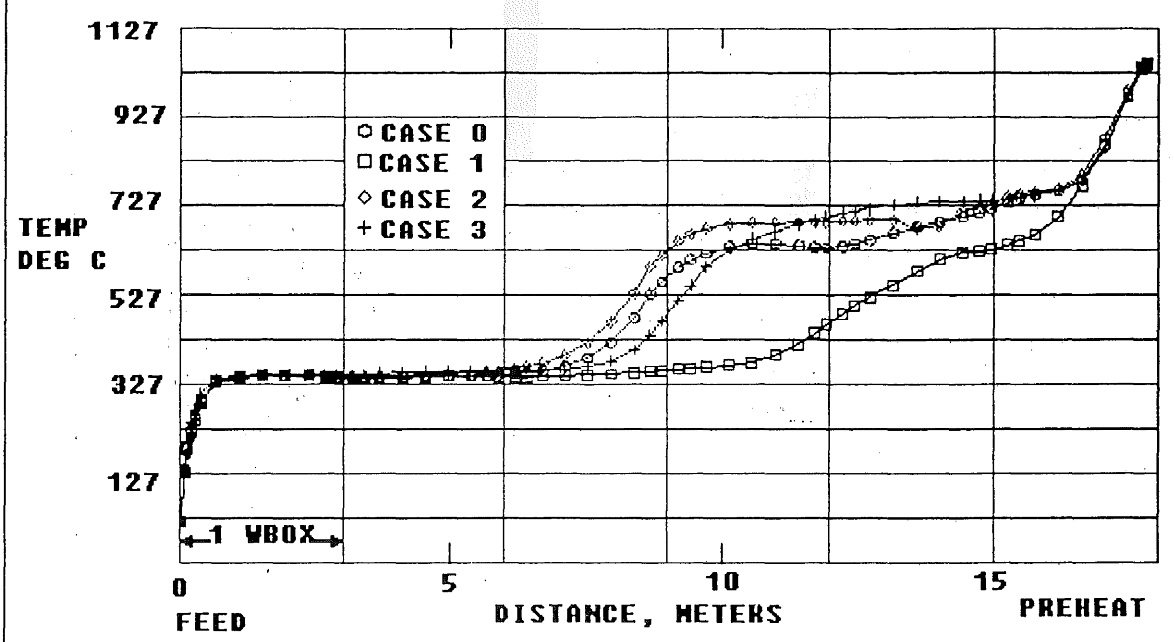

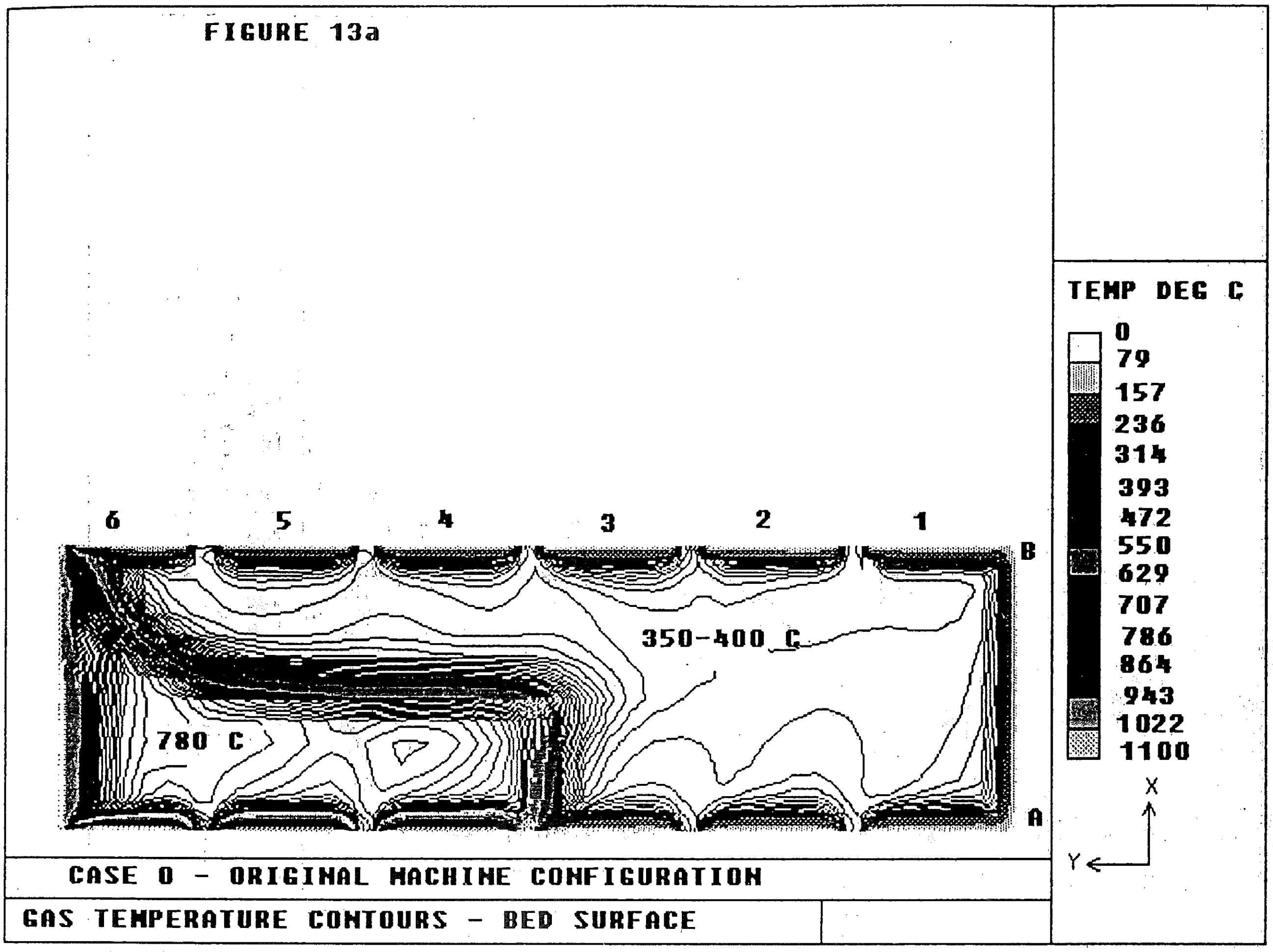
FIGURE 13a
6
5
4
3
2
1
B
A
350-400 C
780 C
TEMP DEG C
0
79
157
236
314
393
472
550
629
707
786
864
943
1022
1100
X
Y
CASE 0 - ORIGINAL MACHINE CONFIGURATION
GAS TEMPERATURE CONTOURS - BED SURFACE

FIGURE 13b

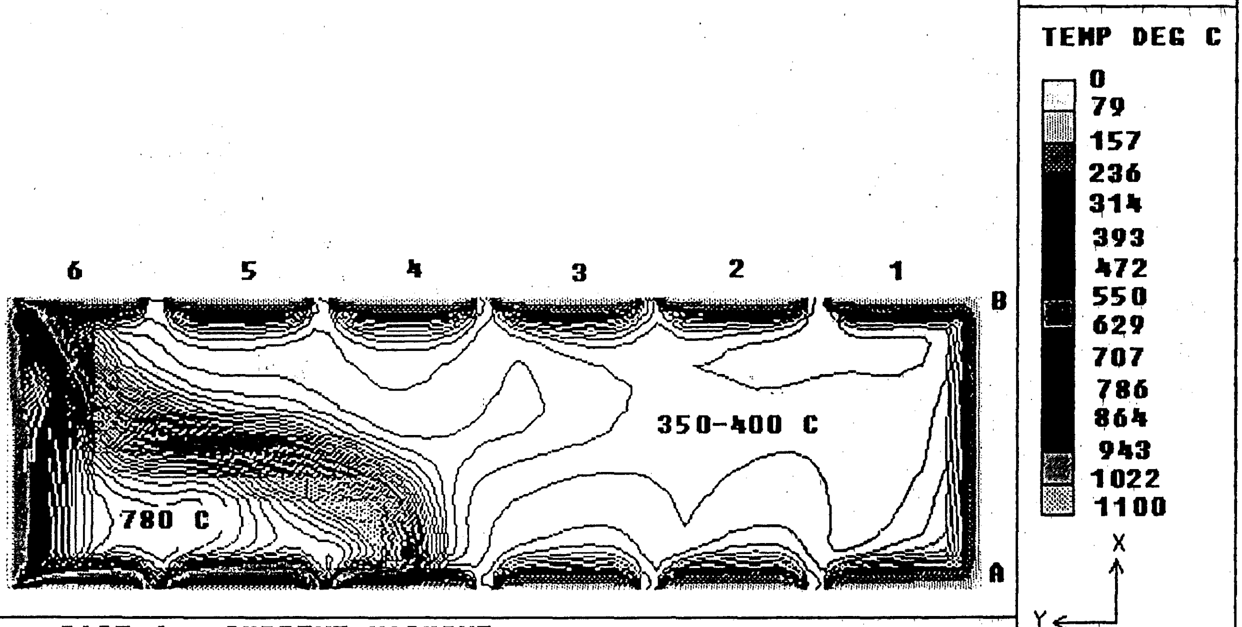

CASE 1 - CURRENT MACHINE

GAS TEMPERATURE CONTOURS - BED SURFACE

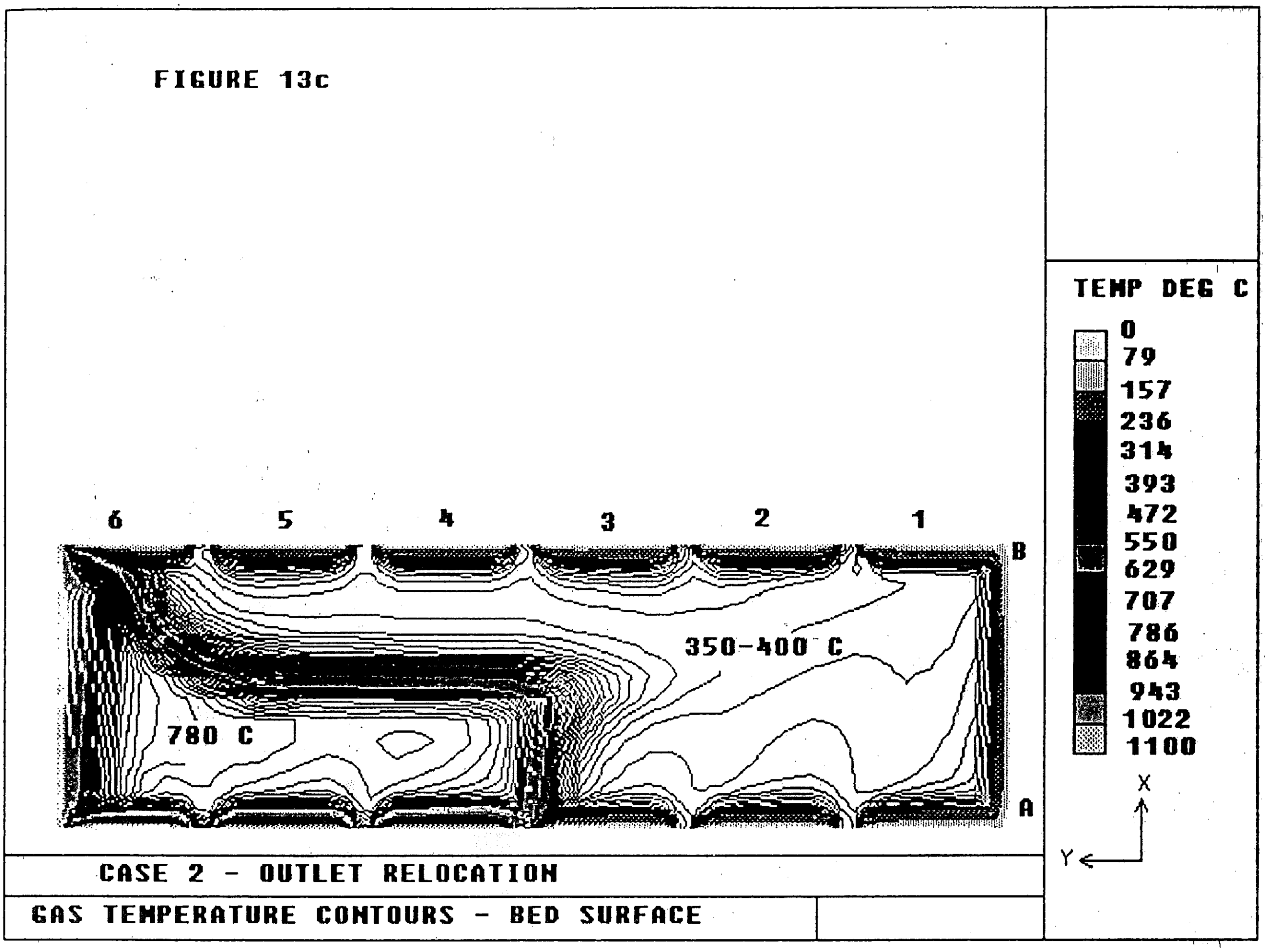
FIGURE 13c
6
5
4
3
2
1
B
A
350-400 C
780 C
TEMP DEG C
0
79
157
236
314
393
472
550
629
707
786
864
943
1022
1100
X
Y
CASE 2 - OUTLET RELOCATION
GAS TEMPERATURE CONTOURS - BED SURFACE

FIGURE 13d

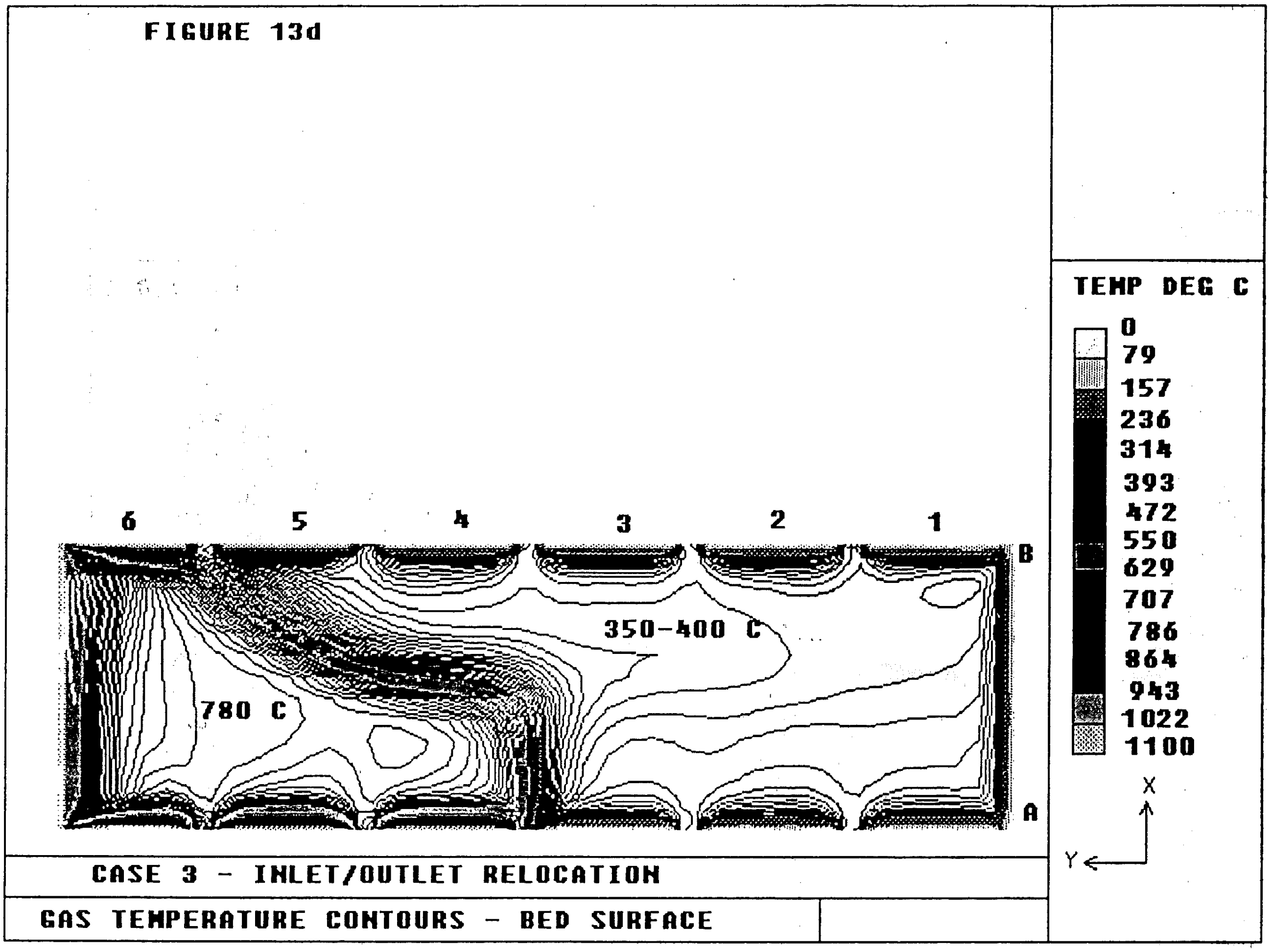

CASE 3 - INLET/OUTLET RELOCATION

GAS TEMPERATURE CONTOURS - BED SURFACE

FIGURE 14
RELATIVE GAS/SOLIDS FLOW

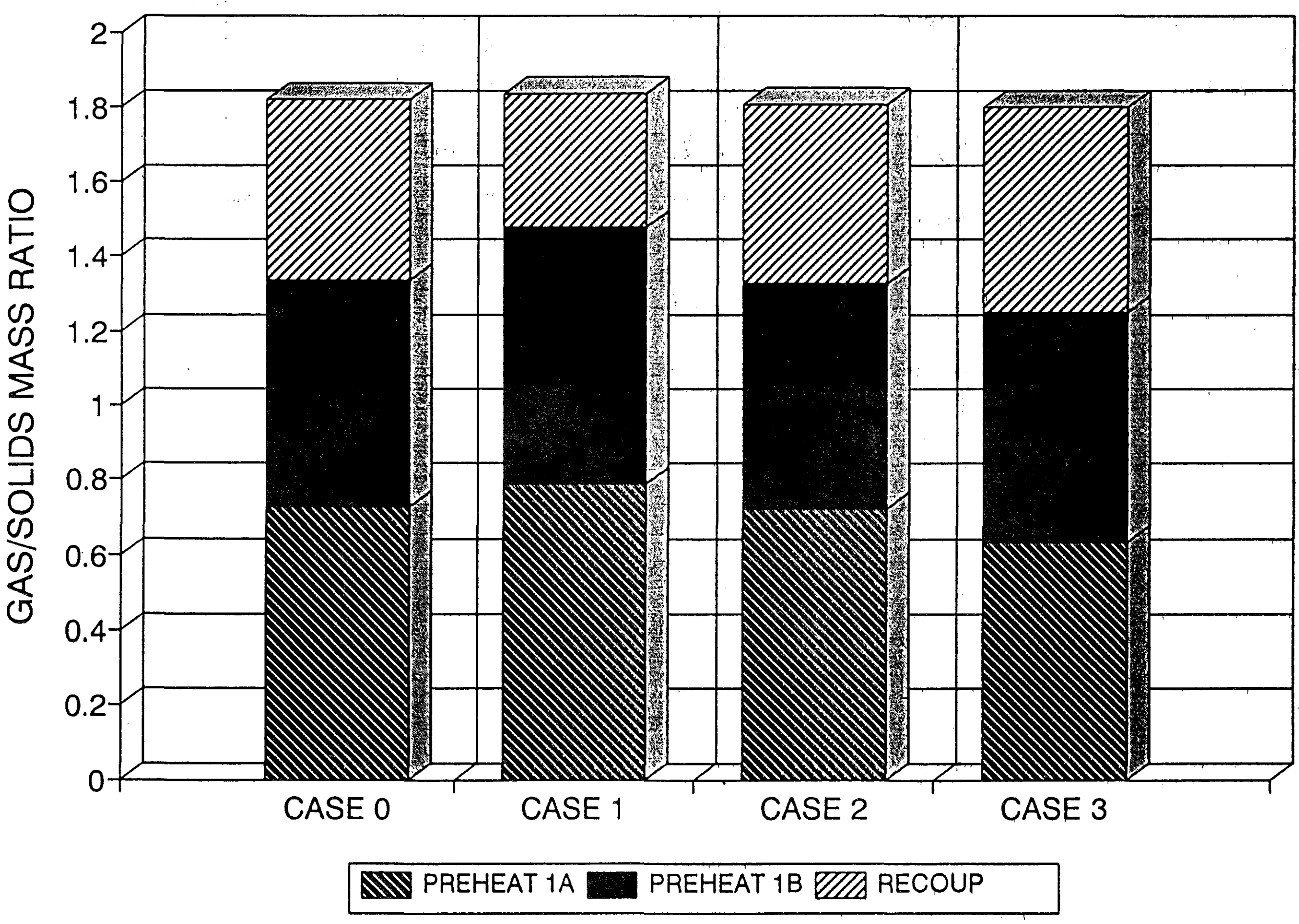

FIGURE 15

GAS TEMPERATURE PROFILES AT BED SURFACE

(POT-GRATE TEST CYCLES)

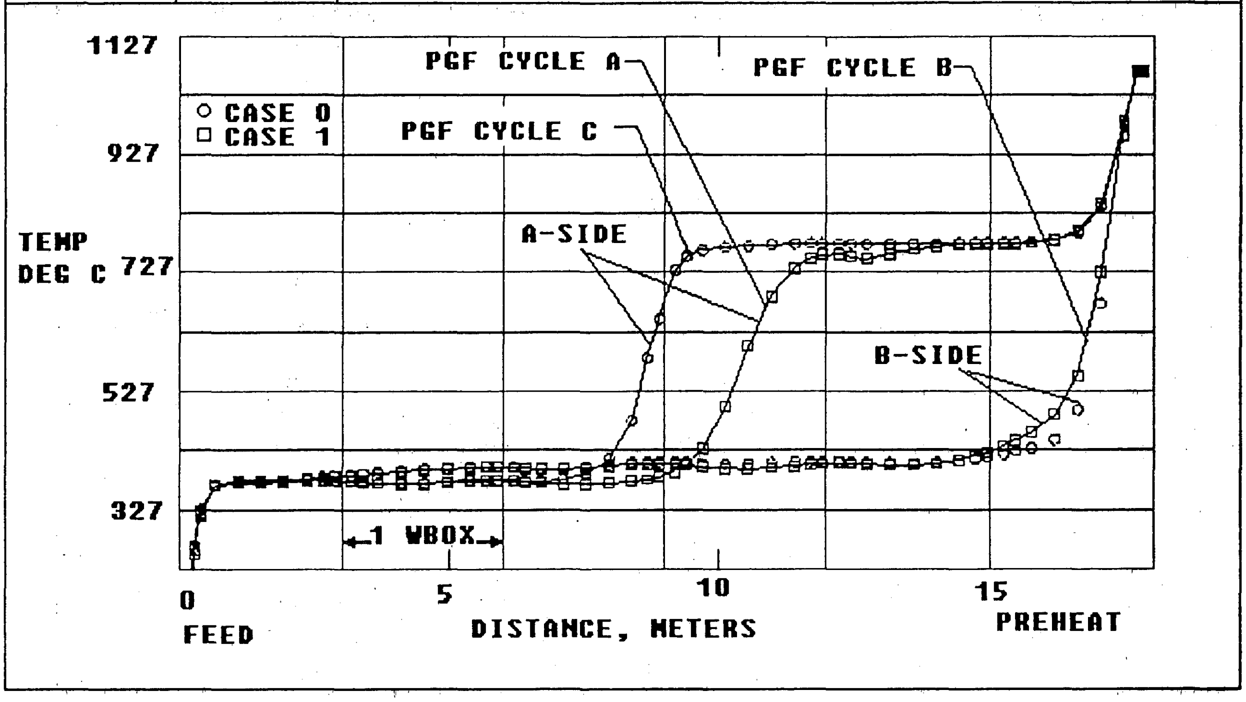

FIGURE 16

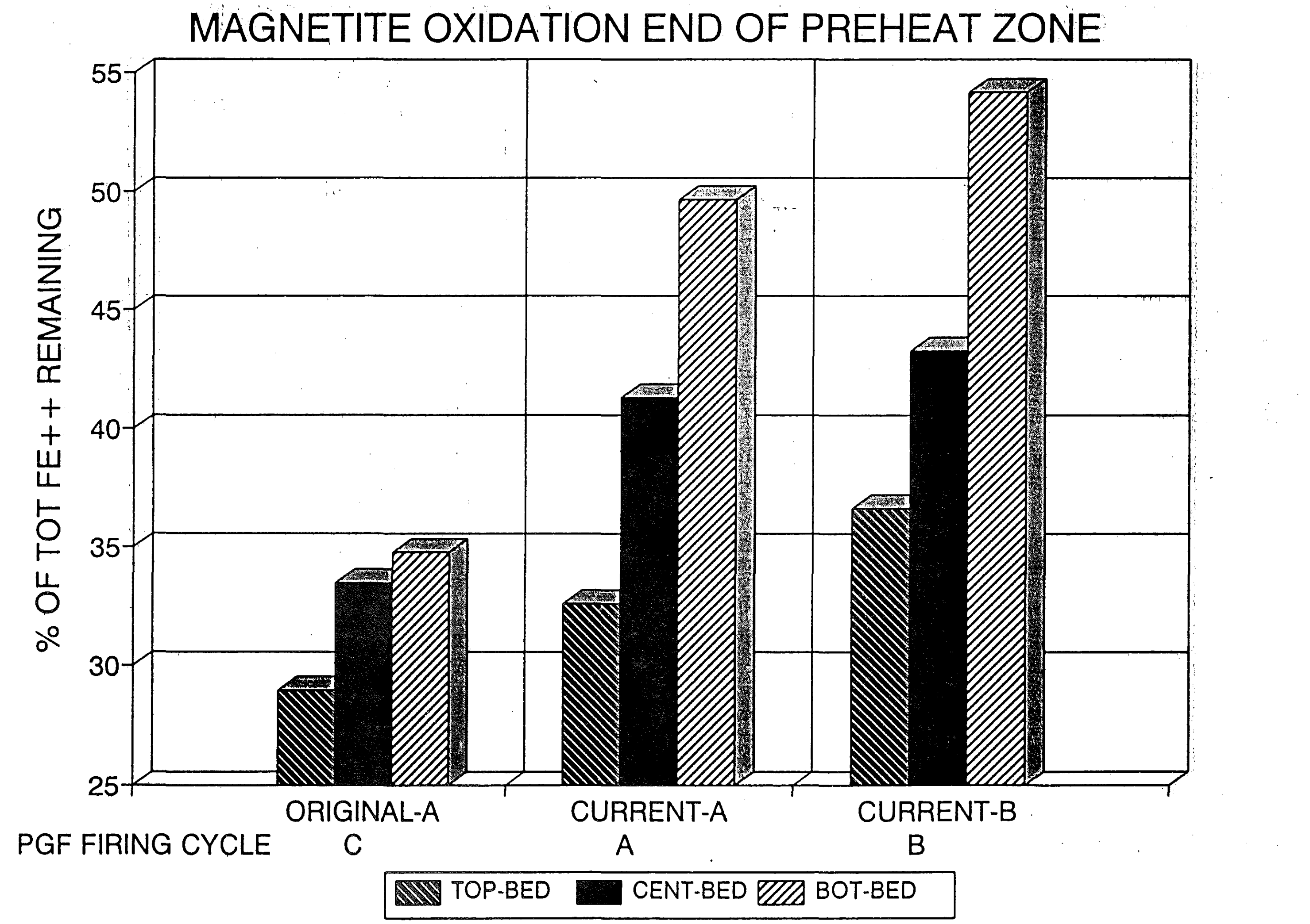
MAGNETITE OXIDATION END OF PREHEAT ZONE
55
50
45
40
35
30
25
% OF TOT FE++ REMAINING
ORIGINAL-A
CURRENT-A
CURRENT-B
PGF FIRING CYCLE
C
A
B
TOP-BED
CENT-BED
BOT-BED

FIGURE 17

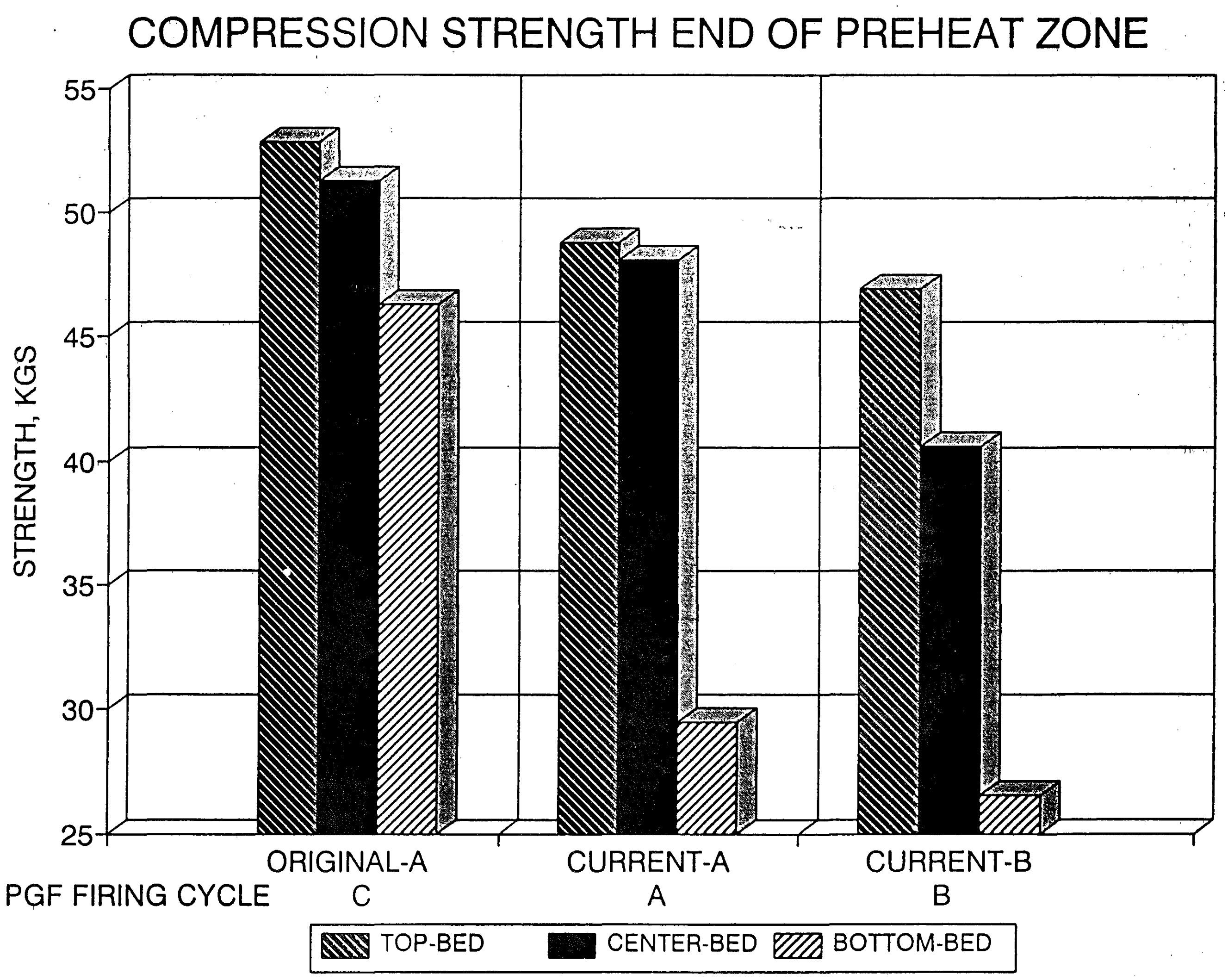
COMPRESSION STRENGTH END OF PREHEAT ZONE
STRENGTH, KGS
55
50
45
40
35
30
25
ORIGINAL-A
CURRENT-A
CURRENT-B
PGF FIRING CYCLE
C
A
B
TOP-BED
CENTER-BED
BOTTOM-BED

FIGURE 18

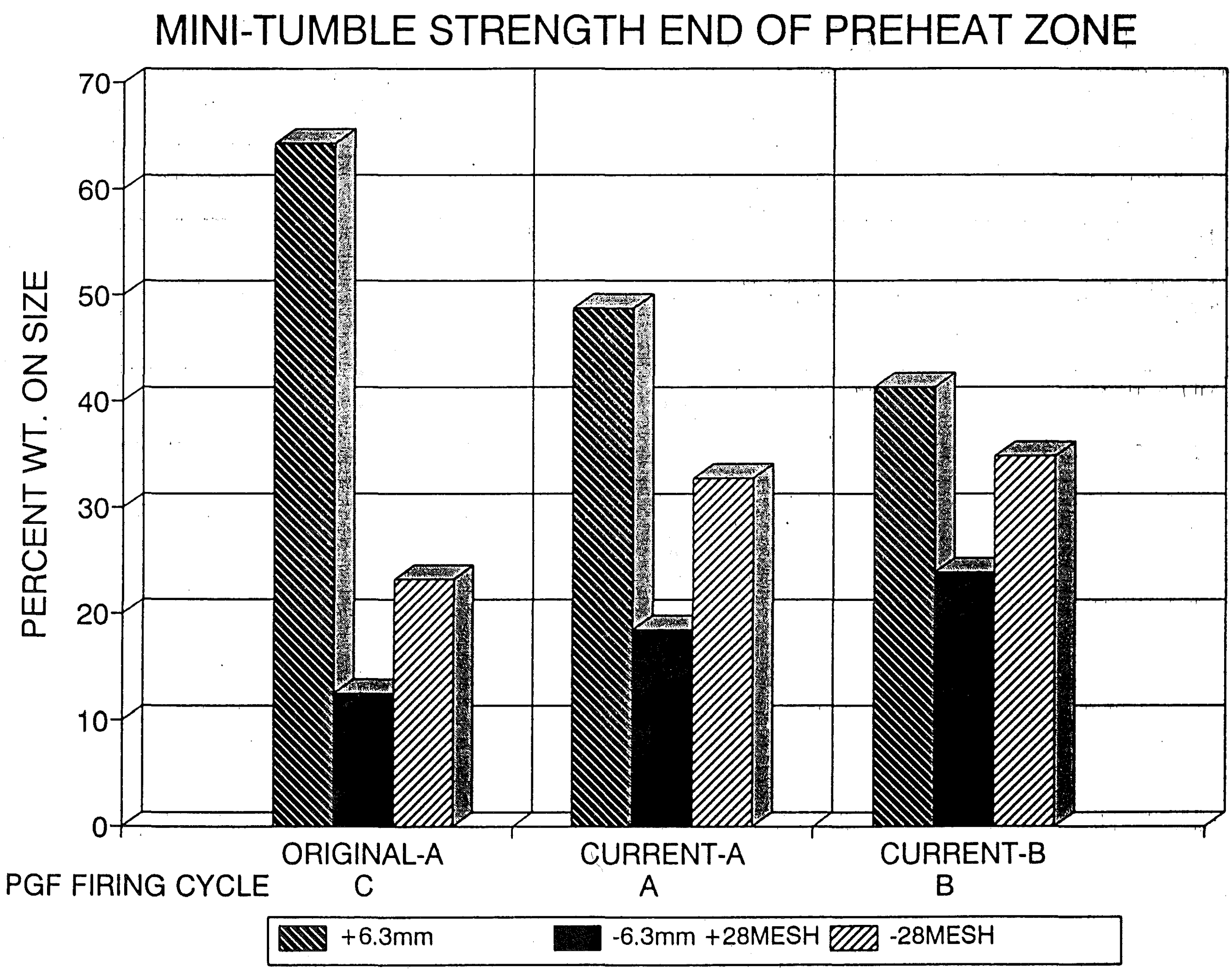
MINI-TUMBLE STRENGTH END OF PREHEAT ZONE
70
60
50
40
30
20
10
0
PERCENT WT. ON SIZE
ORIGINAL-A
C
CURRENT-A
A
CURRENT-B
B
PGF FIRING CYCLE
+6.3mm
-6.3mm +28MESH
-28MESH

FIGURE 19

FIRED PELLET COMPRESSION STRENGTH

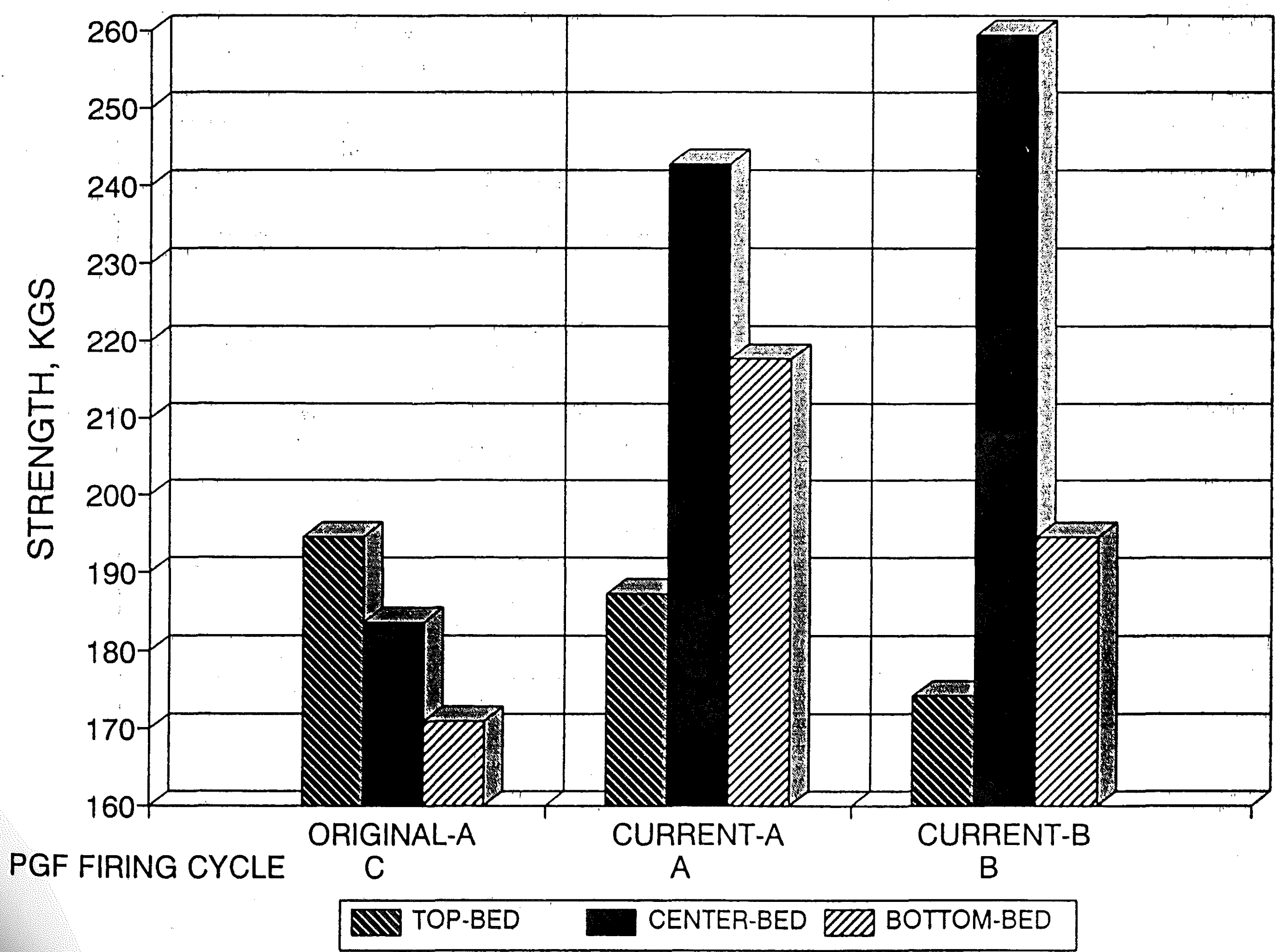

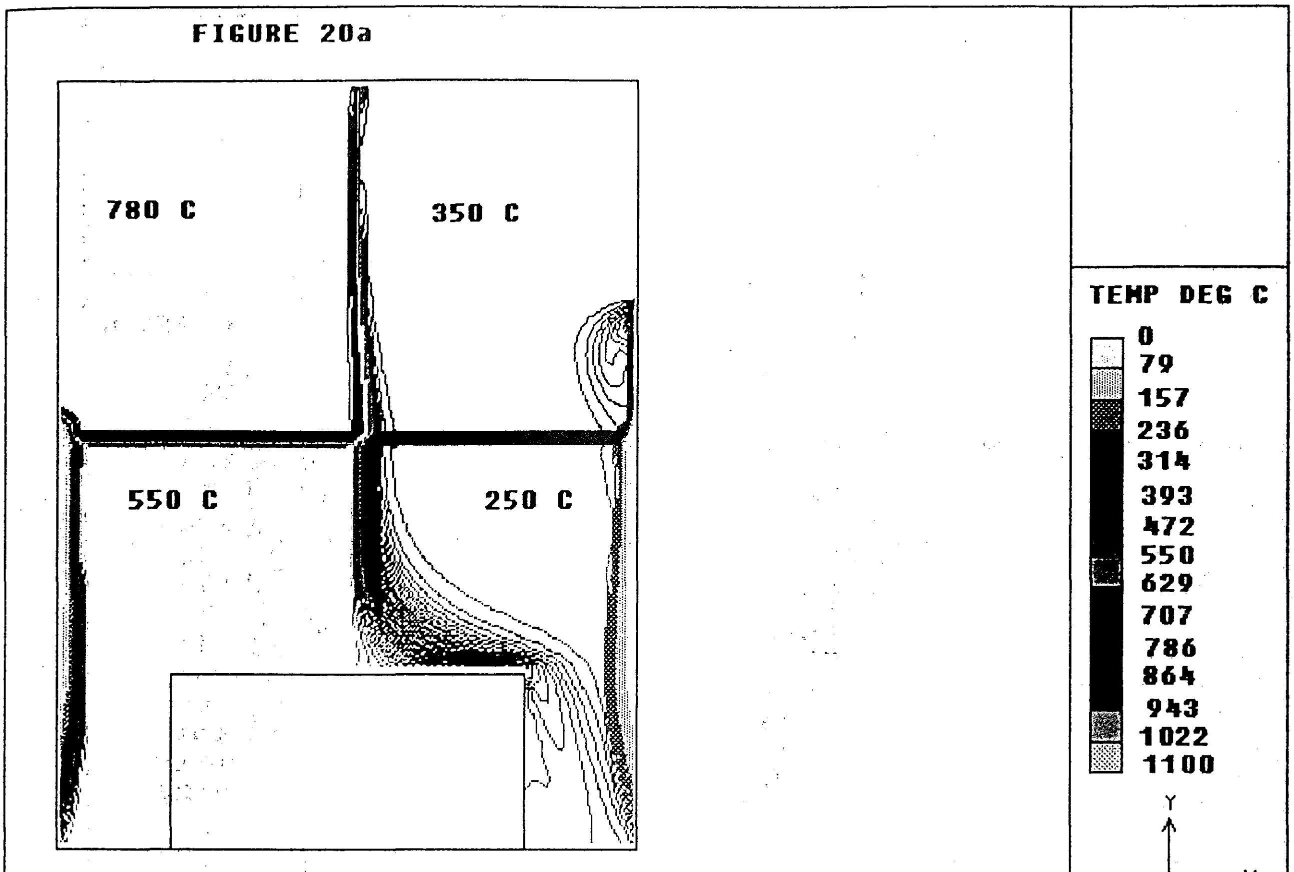

2D MODEL WITHOUT BAFFLE PLATES

GAS TEMPERATURE CONTOURS - WINDBOX 4

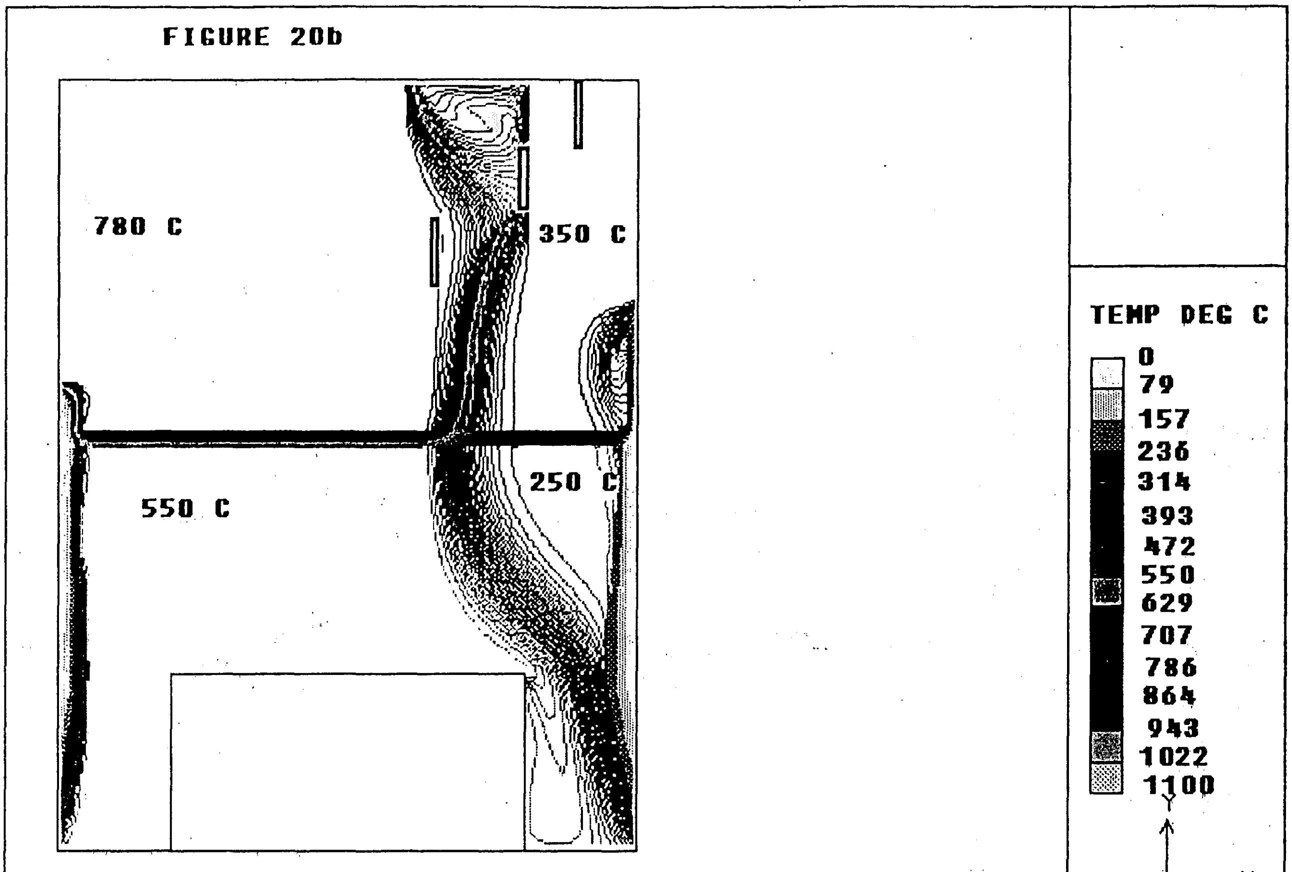

2D MODEL WITH BAFFLE PLATES

GAS TEMPERATURE CONTOURS - WINDBOX 4

FIGURE 21

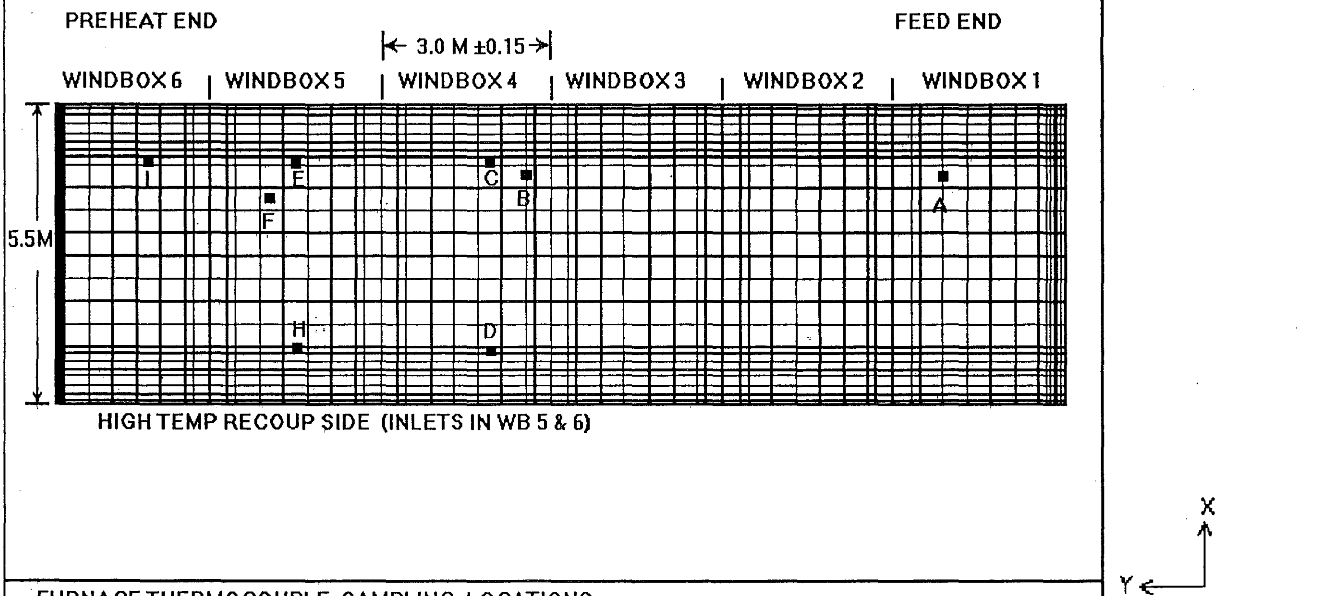

FURNACE THERMOCOUPLE SAMPLING LOCATIONS